N1-Substituent Effects in the Selective Delivery of Polyamine Conjugates into Cells Containing Active Polyamine Transporters

Richard Andrew Gardner,[†] Jean-Guy Delcros,[‡,§] Fanta Konate,[†] Fred Breitbeil III,[†] Bénédicte Martin,[§] Michael Sigman,[†] Min Huang,[†] and Otto Phanstiel IV*,[†]

Groupe de Recherche en Thérapeutique Anticancéreuse and Groupe Cycle Cellulaire,
UMR CNRS 6061 Génétique et Développement, IFR 97 Génomique Fonctionnelle et Santé, Faculté de Médecine,
Université Rennes 1, 2 Av. du Pr Leon Bernard, CS 34317, F-35043 Rennes Cédex, France,
and Department of Chemistry, P.O. Box 162366, University of Central Florida, Orlando, Florida 32816-2366

Several *N*1-arylalkylpolyamines containing various aromatic ring systems were synthesized as their respective HCl salts. The N1-substituents evaluated ranged in size from *N*1-benzyl, *N*1-naphthalen-1-ylmethyl, *N*1-2-(naphthalen-1-yl)ethyl, *N*1-3-(naphthalen-1-yl)propyl, *N*1-anthracen-9-ylmethyl, *N*1-2-(anthracen-9-yl)ethyl, *N*1-3-(anthracen-9-yl)propyl, and pyren-1-ylmethyl. The polyamine architecture was also altered and ranged from diamine to triamine and tetraamine systems. Biological activities in L1210 (murine leukemia), Chinese hamster ovary (CHO), and CHO's polyamine transport-deficient mutant (CHO-MG) cell lines were investigated via IC$_{50}$ cytotoxicity determinations. K_i values for spermidine uptake were also determined in L1210 cells. The size of the *N*1-arylalkyl substituent as well as the polyamine sequence used had direct bearing on the observed cytotoxicity profiles. N1-Tethers longer than ethylene showed dramatic loss of selectivity for the polyamine transporter (PAT) as shown in a CHO/CHO-MG cytotoxicity screen. In summary, there are clear limits to the size of N1-substituents, which can be accommodated by the polyamine transporter. A direct correlation was observed between polyamine-conjugate uptake and cytotoxicity. In this regard, a cytotoxicity model was proposed, which describes a hydrophobic pocket of set dimensions adjacent to the putative PAT polyamine-binding site.

Introduction

Rapidly dividing cells require large amounts of polyamines in order to grow. The native polyamines **1**−**3** shown in Figure 1 exist mainly as polycations at physiological pH. These charged growth factors can be internally biosynthesized and also imported from exogenous sources.[1] Many tumor types have been shown to contain elevated polyamine levels and an activated polyamine transporter (PAT) for importing exogenous polyamines.[1] These range from neuroblastoma, melanoma, human lymphocytic leukemia, colonic and lung tumor cell lines to murine L1210 cells.[1−7] Due to the enhanced cellular need for these amine growth factors and an activated transport system for their import, one can deliver polyamine−drug conjugates to specific cell types.[1−8] This is possible due to particular structural tolerances of the PAT, which allows for import of non-native polyamine constructs.[2−6]

In this regard, numerous *N*-alkylpolyamines have been synthesized with promising anticancer activity.[7] The molecular recognition events involved in polyamine transport have long been known to be sensitive to the distance separating the nitrogen centers as well as to the number of nitrogens present in the molecule.[1−7] However, recent systematic studies of *N*1-(anthracenyl-
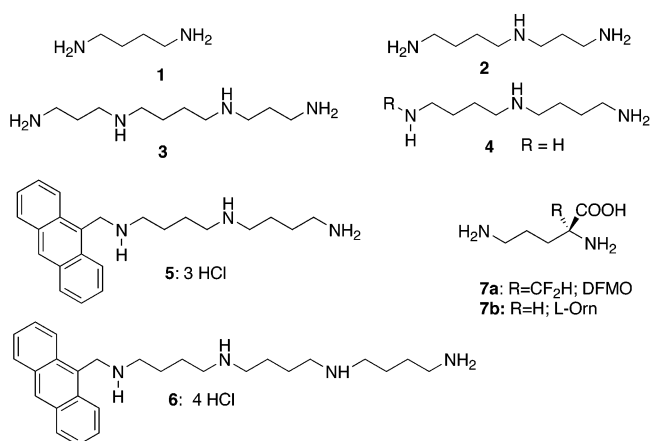

Figure 1. Structures of putrescine **1**, spermidine **2**, spermine **3**, homospermidine **4**, anthracen-9-ylmethyl-4,4-triamine, trihydrochloride **5**, anthracen-9-ylmethyl-4,4,4-tetraamine, tetrahydrochloride **6**, DFMO **7a**, and L-ornithine **7b**.

methyl)polyamines suggested that there are limits to the structural tolerance accommodated by the PAT.[2−6] This report explored the size limitations associated with the N1-substituent and the ability of monosubstituted polyamine systems not only to bind to the PAT but to use the PAT for transport into the cell.

In this report, we focused on the polyamine transporter (PAT). In terms of optimizing polyamine-conjugate design, one must understand the role of both the polyamine component and the appended N-substituent. Our first approach altered the polyamine "message", while maintaining the *N*-anthracen-9-ylmethyl sub-

* Corresponding author. Tel: (407) 823-5410. Fax: (407) 823-2252. E-mail: ophansti@mail.ucf.edu.
† University of Central Florida.
‡ Groupe de Recherche en Thérapeutique Anticancéreuse, University of Rennes 1.
§ Groupe Cycle Cellulaire, University of Rennes 1.

8a: R=H; 2 HCl
8b: R=-(CH$_2$)$_3$NH$_2$; 3 HCl
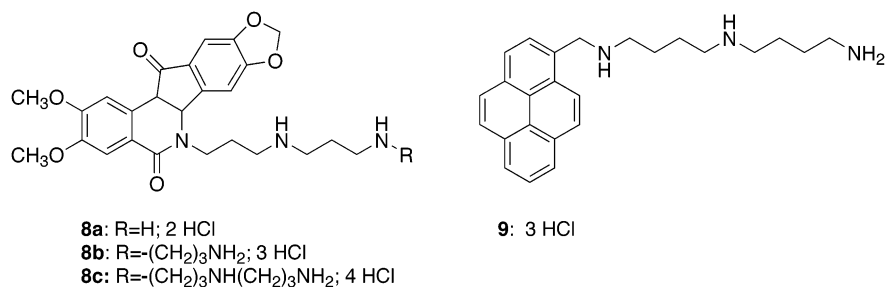**8c**: R=-(CH$_2$)$_3$NH(CH$_2$)$_3$NH$_2$; 4 HCl

9: 3 HCl

Figure 2. Polyamine conjugates **8** and **9**.

stituent (e.g., AntCH$_2$). This approach delineated how various polyamine architectures influenced the delivery of polyamine−anthracene conjugates into cells with active polyamine transporters.[4−6]

The Polyamine. Many N^1-substituted triamine and tetraamine scaffolds were screened in terms of their ability to deliver a toxic anthracene moiety via the PAT to murine leukemia (L1210) cells, Chinese hamster ovary (CHO) cells, and a mutant PAT-deficient CHO cell line (CHO-MG). The homospermidine architecture **4** was shown to be a superior vectoring motif. For example, the N^1-anthracenylmethyl-4,4-triamine **5** (Figure 1) was shown to be nearly 150 times more toxic to CHO cells with high PAT activity than to a CHO-MG mutant, which was PAT-deficient.[4,5] In addition, microscopy studies with detached A375 melanoma cells revealed the rapid uptake of this analogue over its 4,4,4-tetraamine counterpart **6** (Figure 1).[5] This was surprising as the K_i value for **6** (0.051 μM) was approximately 35 times lower than that of **5** (1.8 μM).[4,5] It was suggested that high-affinity PAT ligands, such as **6**, seem to be less efficient vectors and may actually limit their own import into cells by destabilizing cellular membranes.[5] Therefore, at least in the N-alkylaryl systems studied, K_i values were not reliable indicators of polyamine-conjugate transport into the cell and **4** was the more efficacious vector system.[4−6]

While there is a clear preference for the homospermidine motif **4** in the anthracene series, similar preferences may also apply to other polyamine-conjugate systems. For example, in Cushman's recent evaluation of idenoisoquinoline−polyamine conjugates **8** (Figure 2), no significant increase in cytotoxicity was observed through incorporation of additional amino groups in the side chain.[8a] One possible explanation was the use of the 3,3-triamine motif (e.g., **8b**), which was shown to be a nonoptimal vectoring sequence in a related anthracene system.[3]

However, one caveat of the Cushman study was the absence of aminoguanidine (AG) in their NCI-conducted bioassay. Without the presence of an amine oxidase inhibitor like AG, serum amine oxidases may have converted polyamine substrates such as **8** into reactive aldehydes and hydrogen peroxide, making their cytotoxicity profiles unreliable.[8b]

Nevertheless, the authors rationalized their findings by stating that "the optimal use of the polyamine transporter is not open to an indiscriminate array of structural motifs."[8a] This rationale is consistent with the findings of other authors, who have used the polyamine transporter for drug delivery.[1]

Therefore, defining the architectural and physiochemical constraints accommodated by the polyamine

transporter is of clear benefit to future polyamine-conjugate design.

The N-Substituent. Understanding the limits of "cargo" size (i.e., the size of the N^1-substituent), hydrophobicity, and functional groups accommodated by the PAT would facilitate the selection of specific drug classes for attachment and the tethers used for this purpose. Indeed, one could readily imagine attachment of other bioactive agents as the R group in compound **4**[2−6] or onto other polyamine systems (Figure 1).[1−29]

However, there are limitations to this approach. First, not all "cargoes" may be compatible with the PAT-uptake manifold. Second, certain tether lengths may not be accommodated by the PAT. These caveats will be highlighted in this report.

While compounds which enter cells by pathways other than PAT have clear clinical value, designing PAT-selective ligands requires further knowledge of the structural constraints accommodated by the transporter. Encouraged by the selectivity and uptake profile of **5**, we decided to explore the limitations of size accommodated by the N^1-position of the homospermidine vector, **4**.[5]

In a recent report we demonstrated that even an N^1-pyrenylmethyl group could be delivered to CHO cells via conjugation to homospermidine (i.e., **9** in Figure 2), albeit with lower selectivity than an N^1-anthracenylmethyl group.[6] Having shown that the PAT could accommodate relatively large N^1-substituents on **4**, the question arose as to what was the optimal tether length to attach such agents to the polyamine scaffold. Could a large N^1-substituent with a long tether linked to **4** still retain its delivery characteristics and cytotoxicity profile? Thus, we embarked on understanding the sensitivity of the PAT to the alkyl tether separating the N^1-amine center and the appended aryl substituent.

By studying how longer tethers influenced the survival of cells with active and inactive polyamine transport systems, we were able to relate how conjugate architecture influenced cytotoxicity and PAT targeting. By judicious choice of amine substrates (e.g., a homologous series) and proper biological experiments (e.g., IC$_{50}$, K_i, and drug uptake measurements) in selected cell types (murine leukemia L1210, CHO, and CHO-MG cells), a better understanding between polyamine-conjugate structure, transporter affinity, cytotoxicity, and uptake was obtained. Outcomes from these studies led to the development of a new model, which described the relationships between polyamine-conjugate architecture, cytotoxicity, and the structural tolerances accommodated by the polyamine transporter.
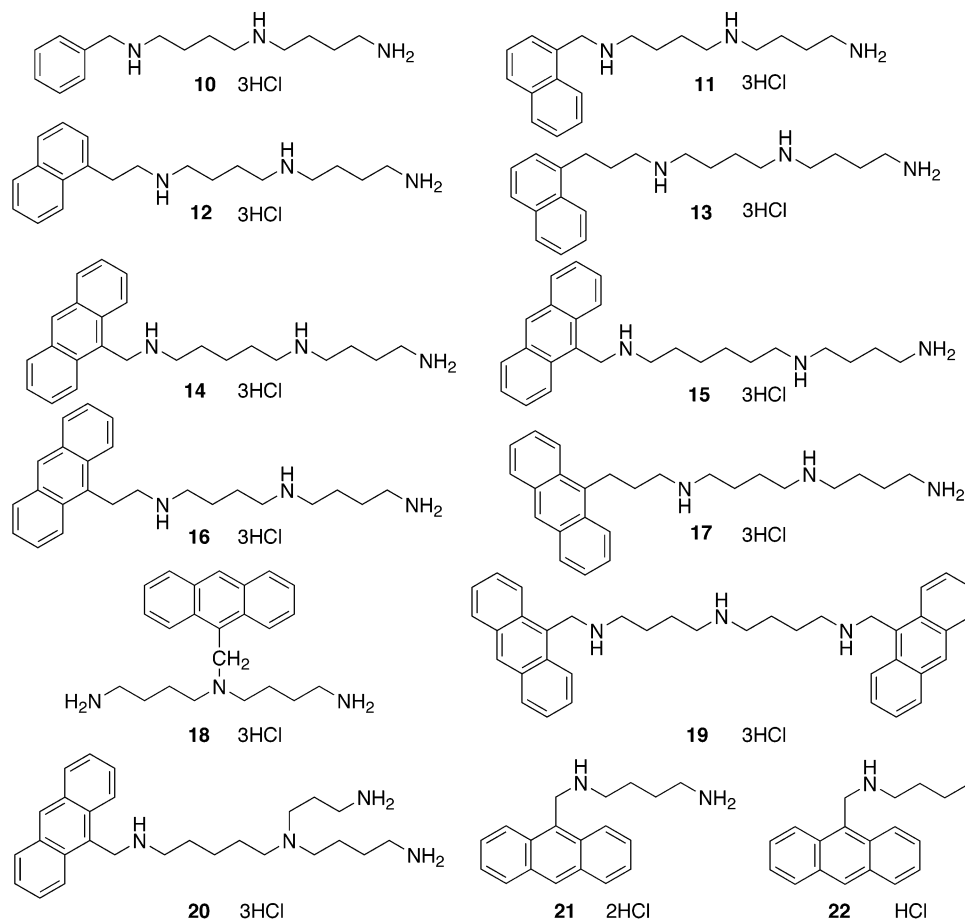
Figure 3. Arylalkyl derivatives **10**−**22**.

Results and Discussion

Synthesis. Several new conjugates were synthesized (Figure 3: **12**, **13**, and **15**−**19**) in order to probe how variations in the N-substituent influenced cytotoxicity and PAT affinity. In addition, other conjugates (**15** and **18**−**20**) were used to address particular structural parameters associated with the proposed cytotoxicity model. For example, **5**, **14**, and **15** were used to describe the nuances surrounding the internal tether, while **12**, **13**, **16**, and **17** probed the distance effects between the N^1-position and the polycyclic aromatic derivative. Compounds **18** and **20** were used to reaffirm that attachment via the N^1-position provided the optimal vectoring motif, while derivative **19** was used to probe the PAT selectivity of a novel bis-substituted system.

The N^1-anthracen-9-ylmethyl unit was selected for alteration to enable direct comparison with the previously prepared polyamine conjugates containing this substituent (Figure 3: **5**, **6**, **14**, and **20**−**22**).[1−5] In addition, anthracene provided a convenient UV "probe" for compound identification and elicited a toxic response from cells upon entry (presumably through DNA coordination).[2,3,30]
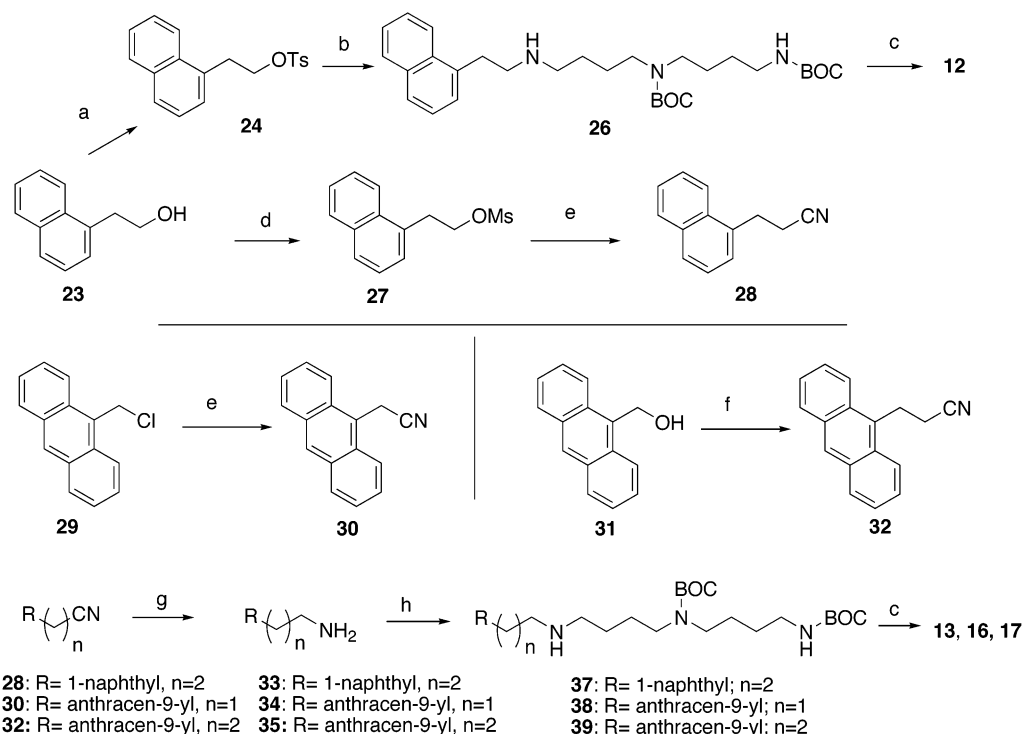
The synthesis of **12**, **13**, and **15**−**19** utilized previously described technology for polyamine synthesis.[2−6,31−33] Compounds **12**, **13**, **16**, and **17** represent homologues of **11** and **5**, where the N^1-tether was sequentially lengthened. As shown in Scheme 1, compound **12** was generated from commercially available alcohol **23** via alkylation of amine **25** with tosylate **24** to give **26**, followed by BOC removal with 4 N HCl. The other conjugates, **13**, **16**, **17**, were synthesized from their respective nitriles: **28**, **30** and **32**. Nitriles **28** and **30** were directly accessed via cyanation of **27** and **29**, respectively. The homologous nitrile **32** was generated in good yield with (cyanomethyl)trimethylphosphonium iodide (2.5 equiv) at 100 °C.[34] As shown at the bottom of Scheme 1, these nitriles were then converted to their respective amines (**33**−**35**) by hydrogenation over Raney nickel followed by alkylation with mesylate **36** to give **37**−**39,** respectively. BOC removal with 4 N HCl provided **13**, **16**, and **17**, respectively.
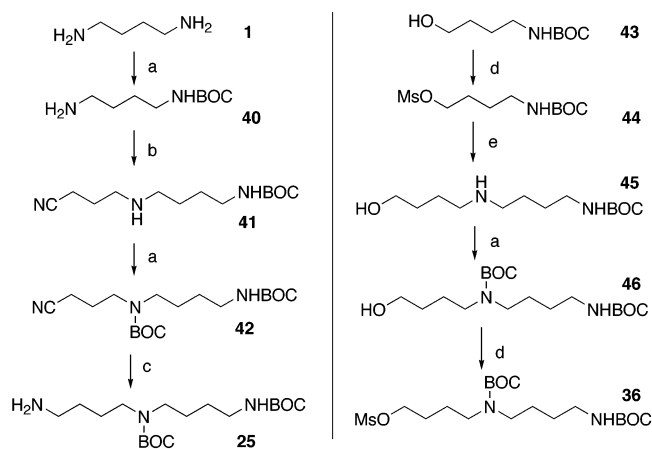
As shown in Scheme 2, the di-BOC protected species **25** and **36** were synthesized via amine alkylation methods. Putrescine **1** was converted to its mono-BOC derivative **40**. Subsequent alkylation with 4-bromobutyronitrile gave the desired secondary amine **41**, which was N-protected with di-*tert*-butyldicarbonate to form **42**. Reduction of the nitrile provided the desired triamine **25**.[35]

An earlier amino-alcohol strategy[31,33] was employed to access mesylate **36**. BOC-protection of 4-aminobutanol gave carbamate **43**, which was then O-sulfonylated to give mesylate **44**. Mesylate displacement with 4-aminobutanol gave the secondary amine **45**, which was then *N*-BOC protected to give **46** and mesylated in successive steps to form **36**.

As shown in Scheme 3, compounds **15**, **18**, and **19** were each generated using the commercially available aldehyde **47**. Synthesis of **15** began with the reductive amination of **47** with 6-aminohexanol to give **48**, followed by *N*-BOC protection to give **49** and O-mesylation

Scheme 1[a]

24
26
12

23
27
28

29
30
31
32

R—(CH)$_n$—CN → R—(CH)$_n$—NH$_2$ → R—(CH)$_n$—NH—...—N(BOC)—...—NH—BOC → **13, 16, 17**

28: R= 1-naphthyl, n=2   **33**: R= 1-naphthyl, n=2   **37**: R= 1-naphthyl; n=2
30: R= anthracen-9-yl, n=1   **34**: R= anthracen-9-yl, n=1   **38**: R= anthracen-9-yl; n=1
32: R= anthracen-9-yl, n=2   **35**: R= anthracen-9-yl, n=2   **39**: R= anthracen-9-yl; n=2

[a] Reagents: (a) TsCl; (b) N^1,N^4-di-BOC homospermidine (**25**, ref 35); (c) 4 N HCl; (d) MsCl; (e) KCN; (f) (cyanomethyl)trimethylphosphonium iodide (2.5 equiv), DIPEA, CH$_3$CH$_2$CN, 100 °C; (g) H$_2$, Raney Ni; (h) MsO(CH$_2$)$_4$N(BOC)(CH$_2$)$_4$NHBOC (**36**).

Scheme 2[a]

H$_2$N—NH$_2$ **1**
H$_2$N—NHBOC **40**
NC—N(H)—NHBOC **41**
NC—N(BOC)—NHBOC **42**
H$_2$N—N(BOC)—NHBOC **25**

HO—NHBOC **43**
MsO—NHBOC **44**
HO—N(H)—NHBOC **45**
HO—N(BOC)—NHBOC **46**
MsO—N(BOC)—NHBOC **36**

[a] Reagents: (a) di-*tert*-butyldicarbonate; (b) 4-bromobutyronitrile; (c) H$_2$, Raney Ni; (d) MsCl; (e) 4-aminobutanol.

to give intermediate **50**. Mesylate **50** was then converted to the triamine **51** and finally to **15**. Compound **18** was generated by reductive amination of **47** with N^1-BOC-1,4-diaminobutane **40** to give the secondary amine **52**, which was then alkylated with 4-bromobutyronitrile to give **53**. Subsequent reduction to the primary amine **54** provided the desired centrally substituted analogue **18** after treatment with 4 N HCl. Finally, the regiospecific reductive amination of **55**[4] with aldehyde **47** provided the bis adduct **56** in good yield. As only one imine intermediate was observed during this reaction, there was a high preference for reaction of the primary amine center in lieu of the more hindered secondary amine in **55**. Finally, compound **56** was converted to the desired bis-anthracenyl derivative **19** using 4 N HCl.

**Biological Evaluation.** Once synthesized, the conjugates were screened for cytotoxicity in L1210, CHO, and CHO-MG cells. L1210 (mouse leukemia) cells were selected to enable comparisons with the published IC$_{50}$ and K_i values for a variety of polyamine substrates.[2–6] CHO cells were chosen along with the mutant cell line CHO-MG in order to comment on selective transport via the PAT.[4–6,12] The results are shown in Table 1.

L1210 IC$_{50}$ and K_i Studies. The IC$_{50}$ values listed in Table 1 represent the concentration of the polyamine conjugate required to reduce the relative cell growth by 50%. The K_i values in Table 1 were determined for [^{14}C]-spermidine uptake and reflect the affinity of the polyamine derivative for the polyamine transporter on the cell surface. With both parameters, one can determine whether high affinity for the transporter (e.g., low K_i value) translated into high cytotoxicity (e.g., low IC$_{50}$ value) etc.

The controls **21** and **22** had moderate cytotoxicity (IC$_{50}$ values: 6.3 and 14.6 μM, respectively) in the L1210 cell line and high respective K_i values (32.2 and 62.3 μM), which reflected their low affinity for the PAT.[6] Prior work had shown that these two control compounds were not PAT-selective and provided a measure of anthracene toxicity, when non-PAT pathways were used for cellular entry.[6]

An interesting insight was gained in the K_i studies in regard to PAT affinity. Since the K_i value of the branched tetraamine **20** was more similar to the triamine **14** than to the linear tetraamine **6**, one can conclude that the K_i value is determined in large part by the number of amino groups aligned in a linear fashion.

A comparison of the benzyl[36] (**10**), naphthylmethyl (**11**), anthracenylmethyl (**5**), and pyrenylmethyl series (**9**) has already been published.[6] In terms of the anthracen-9-yl and 1-naphthyl series studied, the arylmethyl

Scheme 3[a]
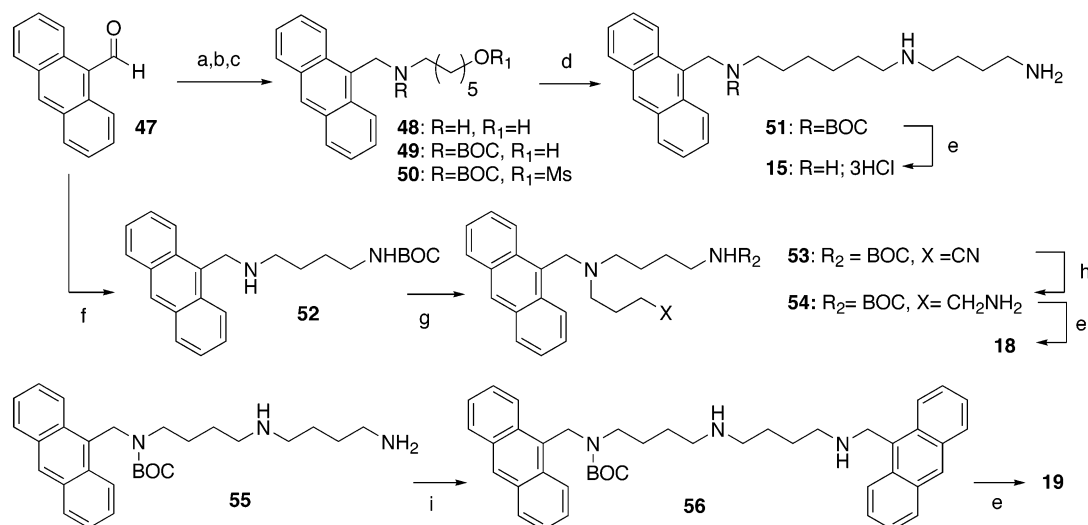
[a] Reagents: (a) 6-aminohexanol, NaBH$_4$; (b) di-*tert*-butyldicarbonate; (c) MsCl; (d) **1**; (e) 4 N HCl; (f) **40**, NaBH$_4$; (g) 4-bromobutyronitrile; (h) H$_2$, Raney Ni; (i) **47**, NaBH$_4$.

Table 1. Biological Evaluation of Polyamine Derivatives in L1210, CHO and CHO-MG Cells[a]

compd (tether)	L1210 IC$_{50}$ (μM)	L1210 K_i values (μM)	ref	CHO-MG IC$_{50}$ (μM)	CHO IC$_{50}$ (μM)	IC$_{50}$ ratio[b]
5: Ant-methyl(4,4)	0.30 ($\pm$0.04)	1.8 ($\pm$0.1)	4	66.7 ($\pm$4.1)	0.45 ($\pm$0.10)	148
6: Ant-methyl(4,4,4)	7.5 ($\pm$0.3)	0.05 ($\pm$0.01)	5	33.2 ($\pm$1.7)	10.6 ($\pm$0.0)	3.1
9: Pyr-methyl(4,4)	0.40 ($\pm$0.02)	2.9 ($\pm$0.3)	6	15.5 ($\pm$2.4)	0.46 ($\pm$0.05)	34
10: benzyl(4,4)	36.3 ($\pm$8.4)	4.5 ($\pm$0.8)	6	>1000	>1000	na
11: Nap-methyl(4,4)	0.50 ($\pm$0.03)	3.8 ($\pm$0.5)	6	>100	0.6 ($\pm$0.2)	>164
12: Nap-ethyl(4,4)	0.53 ($\pm$0.16)	2.0 ($\pm$0.1)		106.1($\pm$11.2)	0.6 ($\pm$0.4)	177
13: Nap-propyl(4,4)	>100	1.3 ($\pm$0.1)		>500[d]	>500[d]	na
14: Ant-methyl(5,4)	0.4 ($\pm$0.1)	1.7 ($\pm$0.2)	4	57.3 ($\pm$2.9)	1.5 ($\pm$0.1)	38
15: Ant-methyl(6,4)	4.1 ($\pm$0.9)	3.5 ($\pm$0.4)		38.2 ($\pm$2.4)	3.0 ($\pm$0.7)	12.7
16: Ant-ethyl(4,4)	3.5 ($\pm$0.7)	1.6 ($\pm$0.1)		33.5 ($\pm$7.1)	9.8 ($\pm$1.1)	3.4
17: Ant-propyl(4,4)	76.3 ($\pm$4.8)	1.1 ($\pm$0.1)		130.8 ($\pm$5.5)	130.1 ($\pm$7.1)	1
18: N^4-Ant-methyl(4,4)	76.7 ($\pm$3.6)	12.7 ($\pm$1.5)		86.6 ($\pm$7.1)	101.8 ($\pm$5.2)	0.9
19: bis N^1,N^9-Ant-methyl(4,4)	1.5 ($\pm$0.1)	4.3 ($\pm$0.2)		1.2 ($\pm$0.1)	1.1 ($\pm$0.1)	1.1
20: Ant-methyl(5,4,3[c])	3.9 ($\pm$1.2)	4.5 ($\pm$0.6)	c	51.3 ($\pm$19.9)	60.9 ($\pm$4.4)	0.8
21: Ant-(butanediamine)	6.3 ($\pm$0.3)	32.2 ($\pm$4.3)	6	7.6 ($\pm$0.4)	7.7 ($\pm$0.5)	1
22: Ant (N-butyl)	14.6 ($\pm$0.1)	62.3 ($\pm$4.2)	4	11.2 ($\pm$2.3)	10.5 ($\pm$2.0)	1.1

[a] Definitions used in Table 1: column 1, Ant = anthracen-9-yl, Nap = 1-naphthyl, Pyr = pyren-1-yl; column 4, ref denotes the reference number in which the data was originally reported; a blank in the ref column denotes new data; column 7, na = not applicable. Cells were incubated for 48 h with the respective conjugate. [b] The ratio denotes the (CHO-MG/CHO) IC$_{50}$ ratio, a measure of PAT selectivity. [c] Derivative **20** is a branched tetraamine, see Figure 3. The synthesis of **20** has been reported in ref 2, and its earlier L1210 47 h IC$_{50}$ value was reported as ~7 μM. The L1210 IC$_{50}$ value was redetermined for consistency. The CHO/CHO-MG data are new for **20**. [d] Forty percent growth inhibition was observed for **13** in both CHO and CHO-MG cell lines. No differential effect was observed.

(**5**, **11**), arylethyl (**12**, **16**), and arylpropyl (**13**, **17**) conjugates provided new insights into the optimal PAT substrate architecture.

First, the K_i values decreased as the tether length increased (e.g., Table 1 K_i values: naphthyl **11**, **12**, **13**, 3.8, 2.0, 1.3 μM; anthracenyl **5**, **16**, **17**, 1.8, 1.6, 1.1 μM, respectively). This is consistent with the longer N^1-tethers having somewhat higher affinity for PAT. A priori one would have thought that higher PAT affinity (lower K_i value) would directly correlate with increased cytotoxicity (lower IC$_{50}$ value). However, neither the above K_i trend nor the one mentioned previously with **5** and **6** correlated with their respective IC$_{50}$ values. In fact, the opposite trend was observed. Therefore, K_i values were of minimal value in predicting the cytotoxicity of these systems.

As the tether was sequentially lengthened within the same series (e.g., **5**, **16**, **17**), the IC$_{50}$ values dramatically increased (0.30, 3.5, and 76.3 μM, respectively)! This

increase in IC$_{50}$ value was also observed within the N^1-naphthylalkyl series (**11**, **12**, **13**), albeit only apparent with the N-propyl chain length (**13**). In short, there was a direct correlation between increased N^1-tether length and higher IC$_{50}$ value (lower cytotoxicity). These collective findings provided the experimental data needed to formulate a cytotoxicity model involving the PAT transporter (see PAT model in Figure 6).

Another interesting trend was apparent in the L1210 IC$_{50}$ values of the series **5**, **14**, and **15**, wherein the polyamine sequence was sequentially modified. Since each compound carried the same anthracenylmethyl group (the toxic component), the differences in IC$_{50}$ were due to the appended polyamine sequence. While the 4,4- and 5,4-triamine systems **5** and **14** gave submicromolar IC$_{50}$ values (0.3 and 0.4 μM, respectively), the 6,4-triamine **15** was 10 fold less toxic (IC$_{50}$ 4.1 μM). This finding is consistent with earlier findings wherein the proper polyamine sequence was required for cellular entry via the polyamine transporter, PAT.

Since triamines have both terminal and internal nitrogen centers, we synthesized the internal Ant derivative **18** to observe whether internal alkylation also provided PAT selective ligands. While Porter et al. had shown that N^4-substituted spermidine (e.g., N^4-hexyl or N^4-benzyl) could still be taken up by the polyamine transporter,[22] the related anthracenylmethyl-homospermidine **18** was over 250-fold less toxic than its N^1-derivative **5** in L1210 cells. This was shown to be due to the lower selectivity of **18** in using PAT for cellular entry and validated our selection of N^1-derivatives for these PAT studies.

The bis analogue **19** was 5-fold less cytotoxic than the monosubstituted 4,4-triamine **5**. Therefore, substitution at both ends of the polyamine chain resulted in a conjugate with lower cytotoxicity. Again, these findings were related to the inability of **19** to selectively use PAT for cellular entry as shown in later CHO studies.

In summary, while the L1210 IC_{50} values allowed comparison to published polyamine systems, the CHO and CHO-MG IC_{50} comparisons were much more informative.

CHO and CHO-MG Studies. CHO cells were chosen along with the mutant cell line CHO-MG in order to comment on how the synthetic conjugates gain access to cells.[4−6,12] The CHO-MG cell line is polyamine-transport-deficient and was isolated after selection for growth resistance to methylglyoxalbis(guanylhydrazone), MGBG, $(CH_3C[=N-NHC(=NH)NH_2]CH[=N-NHC(=NH)NH_2])$ using a single-step selection after mutagenesis with ethylmethanesulfonate.[37,38]

For the purposes of this study, the CHO-MG cell line represents cells with no PAT activity and provided a model for alternative modes of entry or action, which are independent of PAT. These alternative modes of entry include passive diffusion or utilization of another transporter. The alternative modes of action may also include interactions on the outer surface of the plasma membrane or other membrane receptor interactions.

In contrast, the parent CHO cell line represents a cell type with high PAT activity.[37,38] Comparison of conjugate cytotoxicity in these two CHO lines provided an important screen to detect selective conjugate delivery via the PAT. For example, a conjugate with high utilization of the polyamine transporter would be very toxic to CHO cells, but less so to CHO-MG cells.[4−6,12] In short, highly selective PAT ligands should give high (CHO-MG/CHO) IC_{50} ratios.

As shown in Table 1, the controls **21** and **22** had no preference for either CHO cell line with virtually identical IC_{50} values in both CHO-MG and CHO cells. This observation was consistent with **21** and **22** entering the cell through non-PAT mediated pathways.[6] In addition, compounds **17−20** also showed no preference for either CHO cell line.

In contrast, dramatic differences in cytotoxicity were observed with **5** (CHO IC_{50} of **5**, 0.45 μM; CHO-MG/CHO IC_{50} ratio, 148), a highly PAT-selective substrate. Indeed, the CHO-MG/CHO IC_{50} ratios in Table 1 suggested that PAT targeting is influenced by both the polyamine sequence and the appended N^1-substituent. For example, terminal aminobutylation of triamine **5** to give tetraamine **6** significantly reduced its CHO cytotoxicity (CHO IC_{50} of **6**: 10.6 μM, a 24-fold de-

crease)[5] and PAT selectivity (CHO-MG/CHO IC_{50} ratio for **6**: 3.1).

The influence of altering the N^1-substituent was exemplified in two series. First, in terms of the 1-naphthyl series studied, the naphthylmethyl (**11**) and naphthylethyl (**12**) conjugates were highly selective PAT substrates with CHO-MG/CHO IC_{50} ratios >164. However, the naphthylpropyl analogue (**13**) had no PAT selectivity. Thus, an additional methylene group was sufficient to dramatically alter the cytotoxicity profile of **13**. These findings are consistent with a molecular recognition event in PAT-mediated transport.

Second, the trend was even more apparent within the anthracenyl series (**5** and **14−17**). Comparisons of the N^1-alkyl tether effects in **5**, **16**, and **17** revealed a decrease in the CHO-MG/CHO IC_{50} ratio at longer N^1-tether lengths. The conjugates became increasing less toxic to CHO cells as the tether increased from methylene (**5**, CHO IC_{50}: 0.45 μM) to ethylene (**16**, CHO IC_{50}: 9.8 μM) and propylene (**17**, CHO IC_{50}: 130.1 μM). This was also reflected in their respective CHO-MG/CHO ratios: 148, 3.4, and 1. These results could be explained by the longer N^1-tethers facilitating the generation of other conformations or molecular shapes, which move the bulky aryl unit out of a nearby hydrophobic pocket with rigid dimensions.

Short tethers with large aryl groups can be tolerated by PAT. Indeed, a comparison of the benzyl (**10**), naphthylmethyl (**11**), anthracenylmethyl (**5**), and pyrenylmethyl series (**9**) in CHO and CHO-MG cells has already been published.[6] Large N^1-arylmethyl substituents appended to **4** were shown to be selectively imported into cells with PAT activity.[6]

Subtle changes in the distances surrounding the N^1-position also resulted in dramatic changes in cytotoxicity in the CHO cell line. For example, maintaining the terminal anthracenylmethyl moiety, but altering the central alkylene tether length sequentially from butylene (**5**), pentylene (**14**), and hexylene (**15**), resulted in decreasing CHO-MG/CHO IC_{50} ratios. As shown in Table 1, the conjugates became less PAT-selective and incrementally less toxic to CHO cells at longer "central" tether lengths.

Where To Put the Cargo? Comparisons of **5** and **18** revealed that attachment of the anthracenylmethyl "cargo" to the N^1-position (e.g., **5**) provided better PAT selectivity, i.e., higher CHO-MG/CHO IC_{50} ratio. This reconfirmed our selection of the N^1-substituted triamines as optimal PAT vectors, since the N^4-substituted system **18** was not PAT selective (CHO-MG/CHO IC_{50} ratio: 0.9). In addition, N^4-aminopropylation of linear **14** to give branched derivative **20** (Table 1, CHO-MG/CHO IC_{50} ratio: 0.8) obliterated the original PAT selectivity of **14** (IC_{50} ratio: 38). Therefore, the PAT-mediated transport system seems to have little tolerance for bulky substituents at the N^4-position. In contrast the N^1-position can readily tolerate even a pyrenylmethyl unit.[6]

Collectively, these insights gave rise to a new model, which described the optimal polyamine-conjugate motif to utilize the PAT for cellular entry. Before generating this model, however, it was important to first demonstrate that the observed differences in cytotoxicity were due to changes in transport via PAT and not due to
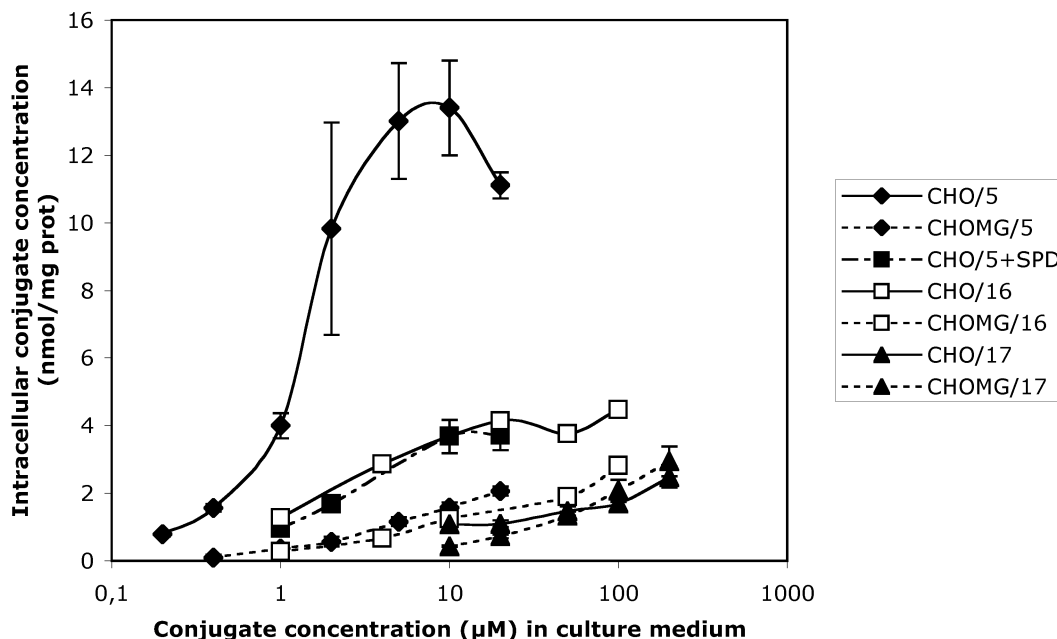
Figure 4. Cell uptake studies with the N^1-(anthracen-9-ylalkyl)homospermidine series (Ant methyl **5**, Ant ethyl **16**, and Ant propyl **17**) in CHO and CHO-MG cells.

intrinsic differences in cytotoxicity. This feature was addressed via transport studies using fluorescent measurements of polyamine conjugates (i.e., **5**, **16**, and **17**) recovered from dosed CHO and CHO-MG cells.

Uptake. In order to relate these compelling IC$_{50}$ trends to actual cell uptake of each conjugate, we performed a series of fluorescence experiments to measure conjugate import. In particular, the "signature" fluorescence profile associated with the anthracene cargo was used to monitor conjugate uptake in CHO and CHO-MG cells (Figure 4). The fluorescence spectra of the anthracene conjugates showed a consistent λ_{max} near 364 nm and emission maxima near 395, 416, and 439 nm. The 416 nm emission band was the most intense of the three observed. Therefore, the anthracene component was easily tracked via its diagnostic fluorescence properties.

In separate experiments run in tandem, CHO and CHO-MG cells were incubated for 24 h with either conjugate Ant-methyl **5**, Ant-ethyl **16**, or Ant-propyl **17**. After cell lysis, the quantity of imported conjugate was determined by fluorescence measurements of the respective perchloric acid extracts (see Experimental Section).

As shown in Figure 4, experiments conducted with the Ant-methyl **5** and Ant-ethyl **16** revealed that more conjugate entered CHO cells, which have active polyamine transporters, than the PAT-deficient CHO-MG cells. This uptake difference was not apparent with the Ant-propyl analogue **17**. Rewardingly, these uptake results are in perfect agreement with the CHO and CHO-MG cytotoxicity trends observed in Table 1.

It is possible that cells could metabolize the dosed polyamine conjugate and convert it into one or more fluorescent metabolites. The presence of other fluorescing species would give spurious results in terms of quantification via total fluorescence. To address this concern, we developed a new liquid chromatography–mass spectrometry (LC–MS) method to isolate and quantify each conjugate (**5**, **16**, and **17**). Rewardingly, similar results were obtained by this alternative method.

Additional fluorescence experiments were run to demonstrate whether this PAT-mediated process was sensitive to other PAT substrates. Spermidine **2** (SPD, a natural substrate for PAT, 200 μM) was added to CHO cells along with the Ant-methyl derivative **5**. As shown in Figure 4, exogenous spermidine provided a significant "import-inhibition" effect with lower amounts of conjugate **5** entering the cell after 24 h incubation.

As shown in Figure 5, the presence of spermidine also provided cell protection from the polyamine conjugate **5** in two cell lines (L1210 and CHO), but not in the PAT-deficient CHO-MG cell line. The top panel in Figure 5 clearly showed a reduction in cytotoxicity to L1210 cells in the presence of 200 μM spermidine. The lower panel in Figure 5 further illustrated how spermidine protects CHO cells from **5**. This spermidine protection effect has been observed previously[2,3,12] and can be rationalized here by spermidine's competitive access to cells via the PAT. Interestingly, these results also showed that when one prevents **5** from entering cells through PAT, its cytotoxicity effect becomes similar to that observed in CHO-MG cells, which are PAT-deficient. Therefore, both the protection and accumulation studies are in perfect agreement with **5** preferentially using the PAT for cellular entry.

In summary, there is a significant decrease in conjugate uptake via the PAT as the N^1-tether length is increased. Decreased uptake means that less of the drug is inside the cell to exert its cytotoxic effect. Having demonstrated that the cytotoxicity profile of **5**, **16**, and **17** directly correlated with their respective import via PAT, a new model was proposed to summarize these findings.

Model. Other authors have presented models predicated upon structure–activity relationships (SAR) of alkylated polyamine derivatives.[7a,11d] The present work
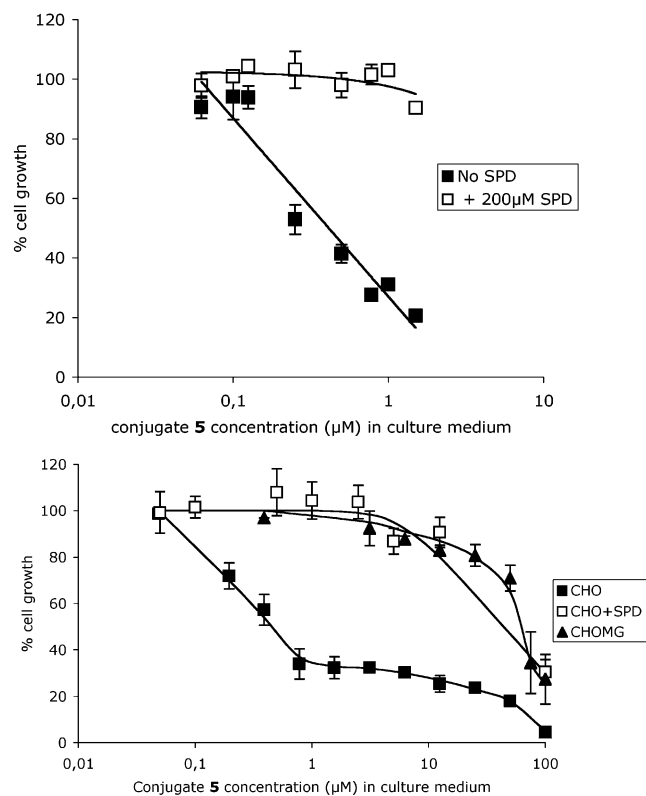
Figure 5. Cytotoxicity of **5** (with and without 200 μM spermidine **2**) in L1210 (top) and CHO/CHO-MG (bottom) cell lines.
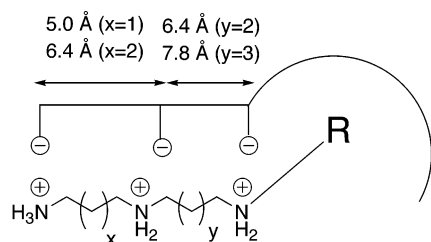

Figure 6. SAR model developed for PAT-selective alkyl-arylpolyamine antitumor agents.

provides a model for estimating the cytotoxicity profile of PAT-selective N^1-substituted triamines.

The experimental results in Table 1, Figures 4 and 5, and prior efforts[2–6] gave rise to a new triamine model (Figure 6). The model will be discussed from left to right. The value of x was optimized in an earlier series of Ant-triamines,[4] where derivatives containing either a propylene ($x = 1$) or a butylene fragment ($x = 2$) had excellent PAT selectivity.[4] Early studies with **5** and **14** coupled with the new findings with **15** provide optimal values for y ($y = 2$ or 3). The size of R in Figure 6 is defined in part by earlier work with the N^1-methylaryl series (**10**, **11**, **5**, and **9**).[6] Considering the significant drop in uptake and cytotoxicity associated in lengthening the methyl tether in **5** to the ethyl tether in **16**, one can estimate the hydrophobic pocket (which accommodates R) to be near the sweep volume of an anthracenylmethyl group.

Other subtleties are present. If R is a smaller group (e.g., naphthyl), one can lengthen the N^1-tether to ethyl and still maintain high PAT selectivity (e.g., **12**). We speculate that the smaller group can still be accommodated by an adjacent hydrophobic pocket of set

Table 2. Distances from N1 to Selected Atoms (Å)

compound	n	N1−H10 (Å)	N1−H3 (Å)
5	1	6.0	6.7
16	2	7.5	7.9
17	3	8.4	8.7

dimensions. However, if the R group is large like the anthracenyl probe in **16** and **17**, small perturbations in the N^1-tether result in a complete loss of PAT selectivity. Note: the pyrenyl probe **9** also indicated the large size accommodated by R pocket, if the short N^1-methyl tether is maintained. Moreover, the value of y in Figure 6 can be either $y = 2$ or $y = 3$ with a large anthracenyl cargo attached and still retain good PAT selectivity (e.g., CHO-MG/CHO IC$_{50}$ ratio of **5**, 148; **14**, 38). However, if the value of y is extended (to $y = 4$) as in **15**, then the PAT selectivity is further diminished (CHO-MG/CHO IC$_{50}$ ratio of **15**: 12.7). Again these results are consistent with a nearby hydrophobic pocket of set dimensions.

Modeling. Using Gaussian 98 augmented with Gaussview, the three systems (**5**, **16**, and **17**) were built and geometry-optimized via computation. The completely staggered model was geometry-optimized using the AM1 semiempirical algorithm. Results were obtained in 10 min. These models were then subjected to a Hartree−Fock optimization using the 3-21G(d) basis set, which each required 2 h to complete.

The distances shown in Table 2 were obtained from these models. The estimated conical height distances (N1−H10) associated with the N^1-substituents in **5**, **16**, and **17** were 6.0, 7.5, and 8.4 Å, respectively. The radius of the cone (H10−H3) remained constant at 4.7 Å. The pertinent distances which define the "sweep triangle" found for **5** were N1−H10, 6.0 Å; H10−H3, 4.7 Å; and H3−N1, 6.7 Å. The approximate volume of the cone swept out by the anthracenyl methyl group in **5** is therefore >100 Å^3. This sweep volume further increased, when the value of n was increased from 1 (e.g., **5**) to 2 (e.g., **16**).

As the tether was sequentially lengthened in **5**, **16**, and **17**, the N1−H3 distance increased by an incremental 1 Å (0.8−1.2Å) with each additional methylene. The putative hydrophobic pocket on the PAT receptor may not be able to accommodate these incremental changes as conjugate import via PAT diminished as the tether was increased (Figure 4).

Since the L1210 K_i values in Table 1 are mostly in the same range (from 4.5 to 1 μM) for all homospermidine-containing conjugates, the N^1-substituent had little effect on PAT affinity in the series studied. In addition, the K_i parameter (a PAT-affinity measure) seemed to be largely determined by the polyamine component, especially in the absence of bulky N^4 substituents (e.g., K_i for **18**: 12.7 μM).

One could rationalize these findings by invoking a two-step model, where first the conjugate binds primarily through its polyamine portion to PAT and then the

Table 3. Cell Selectivity Profile for Ant-methyl **5** and the Ant-*N*-butyl Control **22** (IC_{50} values in μM)

cell type/conjugate	24 h IC_{50}	48 h IC_{50}	72 h IC_{50}
B16 (melanoma)/**5**	1.9 (± 0.1)	1.1 (± 0.1)	0.62 (± 0.03)
Mel-A (normal melanocyte)/**5**	16.5 (± 2.0)	8.3 (± 1.0)	6.5 (± 1.2)
B16 (melanoma)/**22**	19.3 (± 2.8)	21.31 (± 2.18)	20.4 (± 1.8)
Mel-A (normal melanocyte)/**22**	44.3 (± 9.1)	32.80 (± 4.64)	15.0 (± 3.7)

hydrophobic substituent seeks out its associated pocket to initiate the receptor-mediated endocytosis event[6] (or vice versa).

Strategy in Action. Many cancer cell lines are known to have high PAT activity.[6] As shown in Table 3, **5** was 10.5 times more cytotoxic to melanoma B16 cells than to normal melanocytes, Mel-A, after 72 h (e.g., 72 h ratio: 6.5/0.62 = 10.5). The Ant-*N*-butyl control **22**, which has been shown to not use the PAT,[6] showed little selectivity after 72 h (72 h ratio: 15/20.4 = 0.7). While the magnitude of this effect was somewhat time-dependent, conjugate **5** was consistently superior in terms of its ability to target the melanoma cell line.

Since the respective cell doubling times were different, IC_{50} ratios (**22/5**) for each cell type were also compared. This alternative interpretation revealed that the presence of the triamine vector in **5** resulted in 10- to 33-fold higher cytotoxicity in B16 cells, which have high PAT activity, than control **22** (e.g., 72 h ratio: 20.4/0.62 = 33). In contrast, the triamine vector in **5** resulted in only 2- to 4-fold higher cytotoxicity in Mel-A cells than **22** (e.g., 72 h ratio: 15/6.5 = 2.3). To the best of our knowledge, these are the first experiments to demonstrate the PAT-targeting strategy in both normal vs transformed cells.

Conclusions. A series of anthracene−polyamine conjugates were synthesized to probe the sensitivity of the polyamine transporter (PAT) to small structural changes in its substrate. A direct correlation was found between cytotoxicity and the ability of the polyamine conjugate to use the PAT for cellular entry. A survey of these conjugates led to the identification of a general PAT-selective motif, which was effective in targeting the PAT for cellular entry. This motif was illustrated in a new model, which related polyamine−anthracene conjugate structure to PAT-mediated cytotoxicity. Last, this PAT-targeting approach was successfully demonstrated using both a melanoma (B16) and a normal melanocyte cell line (Mel-A).

Experimental Section

Materials. Silica gel (32−63 μm) and chemical reagents were purchased from commercial sources and used without further purification. All solvents were distilled prior to use. ^{1}H and ^{13}C NMR spectra were recorded at 300 and 75 MHz, respectively. TLC solvent systems are based on volume percent, and NH_4OH refers to concentrated aqueous NH_4OH. Elemental analyses were performed by Atlantic Microlabs (Norcross, GA). High-resolution mass spectrometry was performed at the University of Florida Mass Spectrometry facility.

Biological Studies. Murine leukemia cells (L1210), CHO, CHO-MG, B16, and Mel-A cells were grown in RPMI medium supplemented with 10% fetal calf serum, glutamine (2 mM), penicillin (100 unit/mL), and streptomycin (50 μg/mL). L-Proline (2 μg/mL) was added to the culture medium for CHO-MG cells. Cells were grown at 37 °C under a humidified 5% CO_2 atmosphere, except B16 and Mel-A cells, which were grown under 10% CO_2. Aminoguanidine (2 mM) was added to the culture medium to prevent oxidation of the drugs by the enzyme (bovine serum amine oxidase) present in calf serum. Trypan blue staining was used to determine cell viability before the initiation of a cytotoxicity experiment. L1210 cells in early to mid log-phase were used.

IC_{50} Determinations. Cell growth was assayed in sterile 96-well microtiter plates (Becton-Dickinson, Oxnard, CA). L1210 cells were seeded at $5e^4$ cells/mL of medium (100 μL/well). CHO and CHO-MG cells were plated at $2e^3$ cells/mL. B16 cells and Mel-A cells were plated at $7e^2$ and $5e^3$ cells/mL, respectively. Drug solutions (10 μL/well) of appropriate concentration were added at the time of seeding for L1210 cells and after an overnight incubation for the other cells. After exposure to the drug for 48 h, cell growth was determined by measuring formazan formation from 3-(4,5-dimethylthiazol-2-yl)2,5-diphenyltetrazolium using a Titertek Multiskan MCC/340 microplate reader for absorbance (540 nm) measurements.[39] For B16 and Mel-A, cell growth was determined after 24 h and 72 h exposure to the respective conjugates.

K_i Procedure. The ability of the conjugates to interact with the polyamine transport system was determined by measuring competition by the conjugates against radiolabeled spermidine uptake in L1210 cells. This procedure was used to obtain the data listed in Table 1. Initially, the K_m value of spermidine transport was determined as previously described.[40]

The ability of conjugates to compete for [^{14}C]spermidine uptake was determined in L1210 cells by a 10 min uptake assay in the presence of increasing concentrations of competitor, using 1 μM [^{14}C]spermidine as substrate. K_i values for inhibition of spermidine uptake were determined using the Cheng−Prusoff equation[41] from the IC_{50} value derived by iterative curve fitting of the sigmoidal equation describing the velocity of spermidine uptake in the presence of the respective competitor.[42,43] L1210 cells were grown and maintained according to established procedures[44] and were washed twice in HBSS prior to the transport assay.

Fluorescence Studies. Culture flasks were seeded at $2e^5$ cells/mL (CHO or CHO-MG) in complete medium containing aminoguanidine. The respective conjugates (as sterile stock solutions in 0.9% NaCl) were added to the flasks 24 h after the initial seeding at sequential doses ranging from 0.01 to 100 μM, respectively. For the spermidine protection experiment with **5** in Figure 5, spermidine **2** (final concentration 200 μM) was added at the same time as the drug addition.

After 24 h incubation, the cells were harvested and washed in cold 0.9% NaCl and then sonicated in 0.8 mL of a 0.2 N $HClO_4$/1 N NaCl solution to facilitate the extraction process and the proteins precipitated. The mixture was stored overnight at 4 °C. The samples were centrifuged (10 min at 3000 rpm) and the supernatant saved for fluorescence analysis, while the remaining pellets were saved to determine protein content using the Lowry method[45] after dissolution in 0.1 N NaOH.

The quantity of conjugate was determined by fluorescence measurements using calibration curves predetermined with pure material in the 0.2 N perchloric acid/1 N NaCl solution. The excitation and emission maximal wavelengths were slightly different between **5**, **16**, and **17** in 0.2 N $HClO_4$/1 N NaCl. The excitation maximal wavelengths for **5**, **16**, and **17** were 365, 368, and 369 nm, respectively. Emission maxima were at 395, 416, and 439 nm for derivatives **5** and **17**, while **16** had emission maxima at 391, 413, and 436 nm. Therefore, calibration curves allowed for quantification of conjugate import by quantifying the relative fluorescence emissions at these distinctive frequencies and using the predetermined excitation wavelengths. The overall import results are expressed as nanomoles of conjugate/milligram of protein.

LC−MS Method. An Agilent Eclipse XDB-C8 (5 μm, 4.6 × 150 mm) column was used eluting with 25% acetonitrile in water with 0.1% trifluoroacetic acid (TFA) at a flow rate of 0.2 mL/min. The sample injection size was 5 μL, and compound **5** eluted 16 min after injection. Compounds **16** and **17** were eluted using 50% acetonitrile in water with 0.1% TFA (0.2 mL/min) and gave retention times of 8 and 9 min, respectively. Analyses were performed on an Agilent 1100 MSD quadrupole

mass spectrometer equipped with an electrospray ionization (ESI) source and interfaced to an Agilent 1100 HPLC measuring under positive ion mode. The ESI interface was optimized to a capillary voltage of 5 kV, spray chamber temperature of 350 °C, drying gas flow rate of 12.0 L/min, and a nebulizer pressure of 45 psi. The polyamine conjugates were typically observed as $(M + H)^+$. Although a peak at m/z 159 was observed in every sample, it was determined to not be free homospermidine **4** (a potential metabolite) via comparison to an authentic sample of **4**.

N-(4-Aminobutyl)-N′-(2-naphthalen-1-yl-ethyl)butane-1,4-diamine, Trihydrochloride Salt 12. The di-BOC amine **26** (0.08 g, 0.16 mmol) was dissolved in EtOH (1.5 mL) and cooled to 0 °C. HCl (4 N, 2.5 mL) was added dropwise at 0 °C, and the reaction mixture was stirred at room temperature overnight. The solution was concentrated under reduced pressure to give an off-white solid. Absolute EtOH (at 0 °C) was used to wash the solid several times after the solid was initially filtered. The solid was then collected and dried via a vacuum line overnight to give the desired hydrochloride salt **12** as a white solid (0.05 g, 76%). ^{1}H NMR (D$_2$O, 3 drops of DMSO): δ 7.90 (d, 1H), 7.82 (d, 1H), 7.75 (d, 1H), 7.55−7.25 (m, 4H), 3.35 (t, 2H), 3.26 (t, 2H), 2.87 (q, 8H), 1.56 (m, 8H). ^{13}C NMR: δ 133.8, 132.3, 131.1, 129.1, 128.2, 127.5, 127.0, 126.4, 126.0, 123.2, 47.9, 47.1, 39.0, 29.3, 24.2, 23.1, 23.0. HRMS (FAB) calcd for C$_{20}$H$_{32}$N$_3$(M + H): 314.2596. Found: 314.2593. Anal. (C$_{20}$H$_{34}$Cl$_3$N$_3$·0.3H$_2$O) C, H, N.

N-(4-Aminobutyl)-N′-(3-naphthalen-1-yl-propyl)butane-1,4-diamine, Trihydrochloride Salt, 13. The di-BOC amine **37** (0.355 g, 0.67 mmol) was dissolved in absolute ethanol (7 mL) and stirred at 0 °C for 10 min. A 4 N HCl solution (11 mL) was added to the reaction mixture dropwise and stirring continued at 0 °C for 20 min and then at room temperature overnight. The ethanol and aqueous HCl were removed in vacuo, and coevaporation with benzene (5 mL) gave an off-white solid. The solid was suspended in cold ethanol (0 °C, 2 mL), filtered, and then washed several times with cold ethanol. The pure product **13** was obtained as a white powder (0.236 g, 80%). ^{1}H NMR (300 MHz, D$_2$O): δ 7.95 (d, 1H), 7.80 (d, 1H), 7.69 (d, 1H), 7.43 (m, 2H), 7.33 (t, 1H), 7.27 (d, 1H), 3.04 (t, 2H), 2.87 (m, 10H), 1.90 (quin, 2H), 1.55 (m, 8H). ^{13}C NMR: δ 136.7, 133.7, 131.2, 129.0, 127.2, 126.6, 126.2, 126.0, 123.6, 47.4, 47.1, 47.0, 46.9, 39.0, 29.2, 26.7, 24.2, 23.02, 22.98. HRMS (FAB) m/z calcd for C$_{21}$H$_{34}$N$_3$ (M + H)$^+$: 328.2753. Found: 328.2745. Anal. (C$_{21}$H$_{36}$N$_3$Cl$_3$) C, H, N.

N-(4-Aminobutyl)-N′-anthracen-9-ylmethyl-hexane-1,6-diamine, Trihydrochloride Salt, 15. A solution of the mono-BOC diamine **51** (0.48 g, 1 mmol) was dissolved in absolute ethanol (10 mL) and stirred at 0 °C for 10 min. A 4 N HCl solution (15 mL) was added to the reaction mixture dropwise and stirring continued at 0 °C for 20 min and then at room temperature overnight. The ethanol and HCl were removed in vacuo, and coevaporation with benzene (5 mL) gave a yellow solid. The solid was suspended in cold absolute ethanol (0 °C, 2 mL), filtered, and then washed several times with cold ethanol. The pure product **15** was obtained as a yellow solid (0.37 g, 76%). ^{1}H NMR (300 MHz, D$_2$O): δ 8.22 (s, 1H), 7.88 (m, 4H), 7.56 (m, 2H), 7.47 (m, 2H), 4.66 (s, 2H), 3.02 (m, 8H), 1.72 (m, 4H), 1.62 (m, 4H), 1.31 (m, 4H). ^{13}C NMR: δ 130.6, 130.3, 130.0, 129.4, 127.6, 125.5, 122.5, 120.5, 47.74, 47.67, 47.0, 42.5, 39.0, 25.6, 25.43, 25.39, 24.2, 23.0. HRMS (FAB) m/z calcd for C$_{25}$H$_{36}$N$_3$ (M + H)$^+$: 378.2909. Found: 378.2922. Anal. (C$_{25}$H$_{38}$Cl$_3$N$_3$·0.1H$_2$O) C, H, N.

N-(4-Aminobutyl)-N′-(2-anthracen-9-yl-ethyl)butane-1,4-diamine, Trihydrochloride Salt, 16. The di-BOC amine **38** (0.16 mmol) was dissolved in EtOH (0.17 mL) and cooled to 0 °C. HCl (4 N, 0.27 mL) was added dropwise at 0°C. A gummy paste formed after 30 min, which eventually dissolved upon stirring at room temperature overnight. The solution was concentrated under reduced pressure to give a tan solid. Absolute EtOH (at 0 °C) was used to wash the solid several times after the solid was initially filtered. The solid was then collected, and it was dried via a vacuum line overnight to give the desired hydrochloride salt **16** (78%). ^{1}H NMR (300 MHz,

D$_2$O): δ 8.34 (s, 1H), 8.08 (d, 2H, J = 8.8 Hz), 7.96 (d, 2H, J = 8.2 Hz), 7.48. (m. 4H), 3.81 (t, 2H, J = 8.2 Hz), 3.21 (t, 2H, J = 8.2 Hz), 2.98 (m, 8H), 1.68 (m, 8H). ^{13}C NMR (D$_2$O): δ 131.2, 129.5, 129.4, 127.5, 127.0, 125.6, 123.3, 47.5, 47.2 (2C), 47.1, 39.1, 24.2, 24.1, 23.1, 23.0. HRMS theory for C$_{24}$H$_{34}$N$_3$: 364.2753. Found: 364.2745. Anal. (C$_{24}$H$_{36}$N$_3$Cl$_3$·1H$_2$O) C, H, N.

N-(4-Aminobutyl)-N′-(3-anthracen-9-yl-propyl)butane-1,4-diamine, Trihydrochloride Salt, 17. A solution of di-BOC amine **39** (0.13 g, 0.22 mmol) was dissolved in absolute ethanol (3 mL) and stirred at 0 °C for 10 min. A 4 N HCl solution (4 mL) was added to the reaction mixture dropwise and stirring continued at 0 °C for 20 min and then at room temperature overnight. The ethanol and HCl were removed in vacuo, and coevaporation with benzene (5 mL) gave a yellow solid. The solid was suspended in cold absolute ethanol (0 °C, 2 mL), filtered, and then washed several times with cold ethanol. The pure product **17** was obtained as a yellow solid (0.07 g, 64%). ^{1}H NMR (300 MHz, D$_2$O): δ 8.12 (s, 1H), 8.01 (d, 2H), 7.79 (d, 2H), 7.35 (m, 4H), 3.38 (t, 2H), 2.85 (m, 8H), 2.75 (t, 2H), 1.90 (quin, 2H), 1.56 (m, 4H), 1.48 (m, 4H). ^{13}C NMR: δ 132.5, 131.2, 129.3, 129.1, 126.4, 126.3, 125.4, 123.9, 47.3, 47.1, 47.0, 46.8, 39.0, 27.1, 24.2, 23.9, 23.01, 22.98, 22.93. HRMS (FAB) m/z calcd for C$_{25}$H$_{36}$N$_3$ (M + H)$^+$: 378.2909. Found: 378.2914. Anal. (C$_{25}$H$_{38}$N$_3$Cl$_3$) C, H, N.

N^1-(4-Aminobutyl)-N^1-anthracen-9-ylmethyl-butane-1,4-diamine, Trihydrochloride Salt, 18. A solution of the mono-BOC amine **54** (0.70 g, 1.6 mmol) was dissolved in absolute ethanol (16 mL) and stirred at 0 °C for 10 min. A 4 N HCl solution (24 mL) was added to the reaction mixture dropwise and stirring continued at 0 °C for 20 min and then at room temperature overnight. The ethanol and HCl were removed in vacuo, and coevaporation with benzene (5 mL) gave a yellow foam. The pure product **18** was obtained as a yellow foam (520 mg, 73%). ^{1}H NMR (300 MHz, D$_2$O): δ 8.52 (s, 1H), 7.99 (t, 4H), 7.57 (t, 2H), 7.45 (t, 2H), 5.10 (s, 2H), 3.08 (t, 4H), 2.72 (t, 4H), 1.61 (m, 4H), 1.38 (quin, 4H). ^{13}C NMR: δ 132.8, 132.41, 132.35, 131.2, 129.7, 127.2, 124.0, 120.9, 58.9, 54.3, 51.3, 25.6, 22.3. HRMS (FAB) m/z calcd for C$_{23}$H$_{32}$N$_3$ (M + H)$^+$: 350.2596. Found: 350.2579. Anal. (C$_{23}$H$_{34}$N$_3$Cl$_3$·1H$_2$O) C, H, N.

N-Anthracen-9-ylmethyl-N′-{4-[(anthracen-9-ylmethyl)-amino]butyl}butane-1,4-diamine, Trihydrochloride Salt, 19. A solution of the mono-BOC diamine **56** (0.19 g, 0.3 mmol) was dissolved in absolute ethanol (3 mL) and stirred at 0 °C for 10 min. A 4 N HCl solution (4.5 mL) was added to the reaction mixture dropwise, and a gummy paste formed after 30 min, which eventually formed a precipitate upon stirring at room temperature overnight. The ethanol and HCl were removed in vacuo, and coevaporation with benzene (5 mL) gave a yellow solid. The solid was suspended in cold absolute ethanol (0 °C, 2 mL), filtered, and then washed several times with cold ethanol. The pure product **19** was obtained as a yellow solid (0.18 g, 93%). ^{1}H NMR (300 MHz, D$_2$O, 6 drops of DMSO): δ 8.58 (s, 2H), 8.15 (d, 4H), 8.02 (d, 4H), 7.58 (t, 4H), 7.47 (t, 4H), 5.14 (s, 4H), 3.15 (t, 4H), 2.85 (t, 4H), 1.66 (m, 4H), 1.53 (m, 4H). ^{13}C NMR (300 MHz, DMSO): δ 132.0, 131.5, 130.5, 129.0, 127.0, 124.3, 122.8, 48.4, 47.6, 43.8, 24.0, 23.7. HRMS (FAB) m/z calcd for C$_{38}$H$_{42}$N$_3$ (M + H)$^+$: 540.3379. Found: 540.3375. Anal. (C$_{38}$H$_{44}$N$_3$Cl$_3$·2.3H$_2$O) C, H, N.

Toluene-4-sulfonic Acid 2-Naphthalen-1-yl-ethyl Ester, 24. A solution of 2-naphthalen-1-ylethanol **23** (0.5 g, 2.9 mmol) in dry pyridine (10 mL) was stirred at 0 °C for 10 min. p-Toluenesulfonyl chloride (TsCl, 8.7 mmol) was added in small portions over 30 min, and the mixture was stirred at room temperature overnight. The majority of pyridine was removed in vacuo, and the residue was dissolved in CH$_2$Cl$_2$ (100 mL) and washed with aqueous HCl solution (3 × 60 mL). The CH$_2$Cl$_2$ layer was dried over sodium sulfate, filtered, and removed in vacuo to give an oily residue. The residue was purified by flash column chromatography (15% EtAc/hexanes) to yield the product **24** as a white solid (0.54 g, 60%), R_f = 0.35 (15% EtAc/hexanes); mp 62−64 °C. ^{1}H NMR (CDCl$_3$): δ 7.80−7.16 (m, 11H), 4.31 (t, 2H), 3.42 (t, 2H), 2.36 (t, 3H). ^{13}C

NMR: δ 144.8, 134.0, 132.8, 132.1, 131.8, 129.9, 129.1, 128.0, 127.9, 127.7, 126.5, 125.9, 125.7, 123.2, 70.2, 32.9, 22.0. HRMS (FAB) calcd for $C_{19}H_{18}O_3S$: 326.0977. Found: 326.0974. Anal. $(C_{19}H_{18}O_3S)$ C, H, N.

(4-*tert*-Butoxycarbonylamino-butyl)[4-(2-naphthalen-1-yl-ethylamino)butyl]carbamic Acid *tert*-Butyl Ester, 26. To a solution of di-BOC amine **25** (0.2 g, 0.6 mmol) in anhydrous acetonitrile (3 mL) being stirred at 0 °C was added dropwise a solution of the tosylate (0.1 g, 0.3 mmol) in anhydrous acetonitrile (2 mL). The reaction mixture was then warmed to room temperature and refluxed overnight. The acetonitrile was removed in vacuo, and the oily residue was dissolved in CH_2Cl_2 (40 mL) and washed with saturated sodium carbonate solution (2 × 25 mL). The aqueous layers were combined and extracted with CH_2Cl_2 (25 mL). The organic layers were combined, dried over anhydrous sodium sulfate, and filtered, and the solvent was removed in vacuo to give a yellow oil. The oil was purified by flash column chromatography (1% NH₄OH/5% MeOH/CHCl₃) to yield the product **26** as a pale yellow oil (0.1 g, 67%), R_f = 0.3 (1% NH₄-OH/5% MeOH/CHCl₃). ¹H NMR (CDCl₃): δ 8.08 (d, 1H), 7.87 (d, 1H), 7.74 (d, 1H), 7.50−7.27 (m, 4H), 4.64 (br s, 1H), 3.32 (t, 2H), 3.30−3.00 (m, 8H), 2.69 (m, 2H), 1.66 (m, 8H), 1.47 (m, 18H). ¹³C NMR: δ 156.2, 155.7, 136.1, 134.1, 132.1, 129.0, 127.2, 126.8, 126.1, 125.8, 125.7, 123.9, 79.5, 50.8, 49.9, 47.3, 40.6, 33.8, 28.9, 28.8, 27.8, 27.6, 26.3, 26.0. HRMS (FAB) calcd for $C_{30}H_{47}N_3O_4$ (M + H): 514.3645. Found: 514.3649. Anal. $(C_{30}H_{47}N_3O_4 \cdot 0.7H_2O)$ C, H, N.

Methanesulfonic Acid 2-Naphthalen-1-yl-ethyl Ester, 27. A solution of 2-(1-naphthyl)ethanol **23** (1.5 g, 8.7 mmol) in anhydrous CH_2Cl_2 (100 mL) and triethylamine (13.1 mmol, 1.84 mL, 1.5 equiv) was cooled to 0 °C. Methanesulfonyl chloride (13.1 mmol, 1.01 mL, 1.5 equiv) was added dropwise and the resulting solution stirred at 0 °C for 4 h. A 1 M NaOH solution (30 mL) was added slowly to quench the reaction and the mixture warmed to room temperature. The aqueous layer was made up to 50 mL with water, and the organic layer was separated off, washed with water (50 mL), and then dried over sodium sulfate. This was filtered and concentrated in vacuo to give a light brown solid **27** (2.17 g, 99%) that could be used in the next step without further purification. R_f = 0.5 (chloroform). ¹H NMR (300 MHz, CDCl₃): δ 7.99 (d, 1H), 7.85 (d, 1H), 7.68 (d, 1H), 7.50 (m, 2H), 7.39 (m, 2H), 4.53 (t, 2H), 3.53 (t, 2H), 2.78 (s, 3H). ¹³C NMR: δ 134.1, 132.3, 132.0, 129.2, 128.2, 127.8, 126.8, 126.1, 125.8, 123.4, 70.0, 37.6, 33.2. Anal. $(C_{13}H_{14}O_3S)$ C, H, N.

3-Naphthalen-1-yl-propionitrile, 28. To a solution of the mesylate **27** (1.00 g, 4 mmol) in anhydrous acetonitrile (40 mL) were added KCN (2.6 g, 40 mmol) and a catalytic amount of 18-crown-6. The reaction mixture was refluxed with stirring for 18 h. The solvent was removed in vacuo and the residue dissolved in CH_2Cl_2 (100 mL) and washed with water (3 × 60 mL). The water layers were combined and extracted with CH_2Cl_2 (60 mL). The CH_2Cl_2 layers were combined, dried over sodium sulfate, filtered, and removed in vacuo to give a yellow oily residue. The residue was purified by flash column chromatography (1:1 hexane:chloroform) to yield the product **28** as a clear oil (0.53 g, 73%), R_f = 0.4 (1:1 hexane:chloroform). ¹H NMR (300 MHz, CDCl₃): δ 7.83 (m, 2H), 7.73 (d, 1H), 7.47 (m, 2H), 7.37 (t, 1H), 7.31 (d, 1H), 3.34 (t, 2H), 2.66 (t, 2H). ¹³C NMR: δ 134.15, 134.08, 131.3, 129.4, 128.4, 126.8, 126.2, 125.9, 122.9, 119.5, 29.2, 18.9. HRMS (FAB) m/z calcd for $C_{13}H_{12}N$ (M + H)⁺: 182.0970. Found: 182.0974. Anal. $(C_{13}H_{11}N)$ C, H, N.

9-(Cyanomethyl)anthracene, 30. Potassium cyanide was dried in a vacuum desiccator at 110 °C for 4 h. 9-Chloromethylanthracene **29** (0.313 g: 1.38 mmol), KCN (0.90 g: 13.8 mmol), and acetonitrile (50 mL) were combined and refluxed for 2 h with stirring. TLC (50% hexane/CHCl₃) revealed complete consumption of **29**. The reaction mixture was cooled to room temperature, filtered, and concentrated by rotary evaporator. The residue was redissolved in CH_2Cl_2 and washed with water. The organic layer was separated, dried over anhydrous Na_2SO_4, filtered, and concentrated to give nitrile

30 as a yellow solid (0.297 g, 99%). R_f = 0.32 in 50% hexane/CHCl₃; mp 158−159 °C. ¹H NMR (300 MHz, CDCl₃): δ 8.42 (s, 1H), 8.10 (d, 2H), 8.01 (d, 2H), 7.60 (dd, 2H), 7.50 (dd, 2H), 4.50 (s, 2H). ¹³C NMR (CDCl₃): δ 131.4, 129.7, 129.5, 128.8, 127.3, 125.3, 123.0, 120.7, 117.9, 16.4.

3-Anthracen-9-yl-propionitrile, 32.[34] The (cyanomethyl)-trimethylphosphonium iodide reagent was prepared by the following method. A 1 M solution of trimethylphosphine in toluene (21 mL, 21 mmol) was diluted with toluene (10 mL) and tetrahydrofuran (10 mL) and cooled to 0 °C under N₂. Iodoacetonitrile (1.45 mL, 20 mmol) was added dropwise with vigorous stirring, and a white solid precipitated. When the addition was finished, the ice bath was removed and stirring was continued at room temperature for 20 h. The mixture was filtered, and the solid was washed with toluene and dried under reduced pressure to yield the reagent as a white solid (4.7 g, 97%). ¹H NMR (300 MHz, CDCl₃): δ 4.06 (d, 2H), 2.06 (d, 9H).

To a mixture of 9-anthracenemethanol **31** (0.685 g, 3.3 mmol) and (cyanomethyl)trimethylphosphonium iodide (2.0 g, 8.2 mmol) were added propionitrile (8 mL) and diisopropyl-ethylamine (DIPEA, 1.72 mL, 9.9 mmol), and the mixture was stirred at 97 °C for 20 h.[34] Water (0.4 mL, 22.2 mmol) was added, and nitrogen was bubbled through the mixture. The reaction mixture was then stirred at 97 °C for a further 20 h. Water (50 mL) and concentrated hydrochloric acid (2 mL) were added, and the mixture was extracted with ethyl acetate (3 × 50 mL). The combined extracts were washed once with brine, dried over sodium sulfate, filtered, and concentrated in vacuo. The residue was purified by flash column chromatography (1:1 hexane:chloroform) to yield the product **32** as an orange solid[34] (0.57 g, 75%), R_f = 0.3 (1:1 hexane:chloroform). ¹H NMR (300 MHz, CDCl₃): δ 8.37 (s, 1H), 8.10 (d, 2H), 7.97 (d, 2H), 7.52 (t, 2H), 7.43 (t, 2H), 3.94 (t, 2H), 2.71 (t, 2H). ¹³C NMR: δ 131.7, 129.8, 129.7, 129.6, 127.7, 126.8, 125.4, 123.4, 119.5, 24.1, 18.5.

3-Naphthalen-1-yl-propylamine, 33. The nitrile **28** (0.5 g, 2.76 mmol) was dissolved in ethanol (30 mL). NH₄OH (3 mL) and Raney nickel (3 g) were added, and ammonia gas was bubbled through the solution for 10 min at 0 °C. The suspension was hydrogenated at 50 psi for 24 h. Air was bubbled through the solution, and the Raney nickel was removed by filtering through a sintered glass funnel, the Raney nickel residue being kept moist at all times. The ethanol and NH₄-OH were removed in vacuo, and the oily residue was dissolved in CH_2Cl_2 and washed with sodium carbonate (10% aqueous, 2 × 50 mL). The organic layer was dried over anhydrous sodium sulfate and filtered and the solvent removed in vacuo to give the product **33** as a light brown oil, which was used in the next step without further purification (0.5 g, 98%). ¹H NMR (300 MHz, CDCl₃): δ 7.99 (d, 1H), 7.89 (d, 1H), 7.65 (d, 1H), 7.43 (m, 2H), 7.33 (t, 1H), 7.25 (d, 1H), 3.05 (t, 2H), 2.72 (t, 2H), 1.82 (t, 2H), 1.30 (bs, 2H, NH₂). ¹³C NMR: δ 138.3, 134.1, 132.0, 129.0, 126.8, 126.1, 126.0, 125.7, 125.6, 124.0, 42.5, 35.0, 30.7. HRMS (FAB) m/z calcd for $C_{13}H_{16}N$ (M + H)⁺: 186.1283. Found: 186.1282. Anal. $(C_{13}H_{15}N \cdot 0.2H_2O)$ C, H, N.

9-(2-Aminoethyl)anthracene, 34. In a thick-walled glass jar compatible with the Parr shaker, nitrile **30** was dissolved in benzene/ethanol (1:1, 32 mL) and concentrated aqueous NH₄OH (1.6 mL) was added along with Raney nickel (1.6 g). Ammonia gas was bubbled for 5 min through the mixture, which was precooled to 0 °C. The yellow mixture was attached to a Parr shaker, and hydrogen gas (75 psi) was introduced after a brief evacuation of the headspace. After 2 h, TLC (**30**: R_f = 0.32 in 50% hexane/CHCl₃) revealed complete conversion of the nitrile. The mixture was filtered and the filtrate concentrated under vacuum to give a yellow solid (306 mg). Column chromatography (1% NH₄OH/MeOH) gave amine **34** (227 mg, 77%). R_f = 0.31 in 1% NH₄OH/MeOH; mp 90−92 °C. ¹H NMR (300 MHz, CDCl₃): δ 8.25 (s and d, 3H), 7.92 (d, 2H), 7.40 (m, 4H), 3.73 (t, 2H), 3.12 (t, 2H), 1.60 (br s, 2H). ¹³C NMR (CDCl₃): δ 131.9, 131.6, 130.1, 129.3, 126.2, 125.7, 124.9, 124.4, 43.6, 32.1.

3-Anthracen-9-yl-propylamine, 35. The nitrile **32** (0.25 g, 1.1 mmol) was dissolved in ethanol (15 mL) and benzene (15 mL). NH$_4$OH (1.5 mL) and Raney nickel (1.5 g) were added, and ammonia gas was bubbled through the solution for 10 min at 0 °C. The suspension was hydrogenated at 50 parr for 20 h. Air was bubbled through the solution, and the Raney nickel was removed by filtering through a sintered glass funnel, the Raney nickel residue being kept moist at all times. The ethanol and NH$_4$OH were removed in vacuo, and the oily residue was dissolved in CH$_2$Cl$_2$ and washed with 10% aqueous sodium carbonate (3 × 25 mL). The organic layer was dried over anhydrous sodium sulfate and filtered and the solvent removed in vacuo to give the product **35** as a yellow oil, which was used in the next step without further purification (0.23 g, 92%). ^{1}H NMR (300 MHz, CDCl$_3$): δ 8.31 (s, 1H), 8.25 (d, 2H), 7.98 (d, 2H), 7.46 (m, 4H), 3.64 (t, 2H), 2.93 (t, 2H), 1.97 (quin, 2H), 1.50 (br s, 2H, NH$_2$). ^{13}C NMR: δ 134.8, 131.8, 129.8, 129.5, 125.9, 125.7, 125.1, 124.6, 42.9, 35.5, 25.7.

Methanesulfonic Acid 4-[*tert*-Butoxycarbonyl-(4-*tert*-butoxycarbonylamino-butyl)amino]butyl Ester, 36. To a solution of the di-BOC alcohol **46** (0.6 g, 1.7 mmol) in CH$_2$Cl$_2$ (40 mL) and triethylamine (0.35 mL, 2.5 mmol) at 0 °C under N$_2$ was added methanesulfonyl chloride (0.29 g, 2.5 mmol) dropwise. The reaction mixture was stirred at 0 °C for 1 h and left to warm to room temperature and stirred overnight under N$_2$. The reaction mixture was then cooled to 0 °C, and a 1 M NaOH solution (20 mL) was added slowly with vigorous stirring. The organic phase was separated from the aqueous phase and washed with water (2 × 70 mL). The organic phase was dried over sodium sulfate, filtered, and concentrated in vacuo to give the product **36** as a pale yellow oil (0.72 g, 99%), which was used in the next step without further purification. R_f = 0.6 (10% acetone/chloroform). ^{1}H NMR (300 MHz, CDCl$_3$): δ 4.59 (br s, 1H, NHCO), 4.24 (t, 2H, CH$_2$O), 3.15 (m, 6H), 3.01 (s, 3H), 1.74 (m, 2H), 1.63 (m, 2H), 1.58−1.37 (m, 22H, 2 × CH$_2$, 6 × CH$_3$).

[4-(3-Naphthalen-1-yl-propylamino)butyl](4-*tert*-butoxycarbonylamino-butyl)carbamic Acid *tert*-Butyl Ester, 37. To a solution of the amine **33** (0.5 g, 2.7 mmol) in anhydrous acetonitrile (20 mL) and triethylamine (0.19 mL, 1.35 mmol) being stirred at 0 °C was added dropwise a solution of the mesylate **36** (0.59 g, 1.35 mmol) in anhydrous acetonitrile. The reaction mixture was then warmed to room temperature and refluxed overnight. The acetonitrile was removed in vacuo, and the solid/oily residue was dissolved in CH$_2$Cl$_2$ (50 mL) and washed with 1 M sodium hydroxide (2 × 25 mL). The aqueous layers were combined and extracted with CH$_2$Cl$_2$ (25 mL). The organic layers were combined, dried over anhydrous sodium sulfate, and filtered, and the solvent was removed in vacuo to give a light brown oil. The oil was purified by flash column chromatography (10% acetone/CHCl$_3$, then change to 5% MeOH/CHCl$_3$) to yield the product as a clear oil **37** (0.38 g, 54%), R_f = 0.3 (5% MeOH/CHCl$_3$). ^{1}H NMR (300 MHz, CDCl$_3$): δ 8.03 (d, 1H), 7.82 (d, 1H), 7.70 (d, 1H), 7.47 (m, 2H), 7.38 (t, 1H), 7.30 (d, 1H), 4.65 (m, 1H, NHCO), 3.10 (m, 8H), 2.72 (t, 2H), 2.60 (t, 2H), 1.84 (quin, 2H), 1.62−1.35 (m, 26H, 4 × CH$_2$, 6 × CH$_3$). ^{13}C NMR: δ 156.2, 155.7, 138.4, 134.0, 132.0, 128.9, 126.8, 126.1, 125.9, 125.73, 125.65, 124.0, 79.5, 50.2, 50.1, 47.2, 47.1, 40.6, 31.3, 31.2, 28.9, 28.8, 27.8, 26.5, 26.3, 26.0. HRMS (FAB) *m/z* calcd for C$_{31}$H$_{50}$N$_3$O$_4$ (M + H)$^+$: 528.3801. Found: 528.3805. Anal. (C$_{31}$H$_{49}$N$_3$O$_4$·0.2H$_2$O) C, H, N.

[4-(2-Anthracen-9-yl-ethylamino)butyl](4-*tert*-butoxycarbonylamino-butyl)carbamic Acid *tert*-Butyl Ester, **38.** The amine **34** (24.2 mg: 0.11 mmol), triethylamine (TEA, 13.9 μL: 0.1 mmol) and mesylate **36** (46 mg: 0.105 mmol) were dissolved in CH$_3$CN (5 mL) and refluxed overnight. The solvent was removed, and column chromatography (90% CHCl$_3$/10% MeOH/10 drops of NH$_4$OH per 100 mL) provided unreacted **34** (8 mg) and the desired adduct **38** as an oil (25 mg: 63% based on recovered **34**). Note: the mesylate **36** was only visible after the eluted TLC (10% acetone/CHCl$_3$) plate was dipped in a KMnO$_4$ solution and allowed to air-dry. The reaction was repeated on a larger scale using 1.6 equiv of amine **34** to 1

equiv of **36** and gave the desired adduct **38** in 50% yield (148 mg). Column chromatography avoided using a sand layer and was performed in two steps: 10% acetone/CHCl$_3$ to first elute any unreacted mesylate, then switched to 4% MeOH/CHCl$_3$ to elute **38**. R_f = 0.24 (4% MeOH/CHCl$_3$). ^{1}H NMR (CDCl$_3$): δ 8.31 (s, 1H), 8.29 (d, 2H), 7.96 (dd, 2H, *J* = 1.2, 8.2 Hz), 7.43 (m, 4H), 4.68 (br s, 1H, NH), 3.83 (t, 2H, *J* = 7.6 Hz), 3.10 (m, 8H), 2.70 (br s, 2H), 2.30 (br s, 1H, NH), 1.70−1.20 (m, 26H). ^{13}C NMR (CDCl$_3$): δ 156.0, 155.6, 131.9, 131.6, 130.0, 129.2, 126.2, 125.7, 124.9, 124.3, 79.3, 77.4, 50.9, 49.8, 47.0, 40.4, 28.7, 28.6, 27.6, 26.2. HRMS: theory for C$_{34}$H$_{50}$N$_3$O$_4$ (M + 1): 564.3801. Found: 564.3794. Anal. (C$_{34}$H$_{49}$N$_3$O$_4$ 2.4 H$_2$O) C, H, N.

[4-(3-Anthracen-9-yl-propylamino)butyl](4-*tert*-butoxycarbonylamino-butyl)carbamic Acid *tert*-Butyl Ester, 39. To a solution of the amine **35** (0.23 g, 1.0 mmol) in anhydrous acetonitrile (10 mL) and triethylamine (0.9 mL, 0.63 mmol) being stirred at 0 °C was added dropwise a solution of the mesylate **36** (0.28 g, 0.63 mmol) in anhydrous acetonitrile. The reaction mixture was then warmed to room temperature and refluxed for 72 h. The acetonitrile was removed in vacuo, and the oily residue was dissolved in CH$_2$Cl$_2$ (40 mL) and washed with 1 M sodium hydroxide (3 × 25 mL). The CH$_2$Cl$_2$ layer was dried over anhydrous sodium sulfate and filtered and the solvent removed in vacuo to give a dark brown oil. The oil was purified by flash column chromatography (10% acetone/CHCl$_3$, then change to 5% MeOH/CHCl$_3$) to yield the product **39** as a yellow oil (0.15 g, 40%), R_f = 0.3 (5% MeOH/CHCl$_3$). ^{1}H NMR (300 MHz, CDCl$_3$): δ 8.31 (s, 1H), 8.25 (d, 2H), 7.96 (d, 2H), 7.44 (m, 4H), 4.65 (m, 1H, NHCO), 3.63 (t, 2H), 3.10 (m, 6H), 2.82 (t, 2H), 2.62 (t, 2H), 2.02 (quin, 2H), 1.62−1.35 (m, 26H, 4 × CH$_2$, 6 × CH$_3$). ^{13}C NMR: δ 156.3, 155.7, 134.7, 131.8, 129.8, 129.4, 125.9, 125.7, 125.0, 124.6, 79.5, 50.3, 50.0, 47.1, 40.6, 31.7, 28.9, 28.8, 27.8, 27.5, 26.3, 26.0. HRMS (FAB) *m/z* calcd for C$_{35}$H$_{52}$N$_3$O$_4$ (M + H)$^+$: 578.3958. Found: 578.3973. Anal. (C$_{35}$H$_{51}$N$_3$O$_4$·0.8H$_2$O) C, H, N.

(4-Aminobutyl)carbamic Acid *tert*-Butyl Ester, 40. 1,4-Diaminobutane (1.76 g, 20 mmol) was dissolved in a solution of triethylamine and methanol (10% TEA in MeOH, 30 mL). A solution of di-*tert*-butyl dicarbonate (1.45 g, 6.6 mmol) in methanol (20 mL) was added dropwise to this mixture with vigorous stirring. The mixture was stirred at room temperature overnight. The methanol and TEA were removed in vacuo to yield an oily residue, which was dissolved in CH$_2$Cl$_2$ (40 mL) and washed with a solution of sodium carbonate (10% aqueous, 3 × 40 mL). The CH$_2$Cl$_2$ layer was dried over anhydrous sodium sulfate and filtered, the solvent removed in vacuo, and the oily residue purified by flash column chromatography (1:10:89 NH$_4$OH:MeOH:CHCl$_3$) to give the product **40** as a clear oil (0.825 g, 66%), R_f = 0.38 (1:10:89 NH$_4$-OH:MeOH:CHCl$_3$). ^{1}H NMR (300 MHz, CDCl$_3$): δ 4.68 (br s, 1H, NHCO), 3.13 (m, 2H), 2.70 (t, 2H), 1.62−1.33 (m, 13H, 2 × CH$_2$, 3 × CH$_3$).

(4-Hydroxy-butyl)carbamic Acid *tert*-Butyl Ester, 43. A solution of 4-aminobutanol (2.0 g, 22.5 mmol) in methanol (42 mL) and triethylamine (8 mL) was cooled to 0 °C and stirred for 10 min. A solution of di-*tert*-butyl dicarbonate (7.35 g, 33.7 mmol) in methanol (20 mL) was added dropwise over 30 min, and the reaction mixture was stirred overnight under N$_2$ at room temperature. The methanol and triethylamine were removed in vacuo, and the oily residue was dissolved in CH$_2$Cl$_2$ (100 mL) and washed with 0.1 N HCl solution (3 × 100 mL). The CH$_2$Cl$_2$ layer was dried over sodium sulfate, filtered, and removed in vacuo to give the product **43** as a clear oil (2.9 g, 68%), which was used in the next step without further purification. R_f = 0.4 (40% acetone/hexane). ^{1}H NMR (500 MHz, CDCl$_3$): δ 4.76 (br s, 1H, NHCO), 3.62 (m, 2H, CH$_2$O), 3.11 (m, 2H, CH$_2$N), 2.49 (m, 1H, OH), 1.55 (m, 4H), 1.41 (s, 9H).

Methanesulfonic Acid 4-*tert*-Butoxycarbonylamino-butyl Ester, 44. To a solution of the alcohol **43** (1.4 g, 7.4 mmol) in CH$_2$Cl$_2$ (130 mL) and triethylamine (1.55 mL, 11 mmol) at 0 °C under N$_2$ was added methanesulfonyl chloride

(1.27 g, 11 mmol) dropwise over 30 min. The reaction mixture was stirred at 0 °C for 1 h and left to warm to room temperature and stirred overnight under N_2. The reaction mixture was then cooled to 0 °C, and a 1 M NaOH solution (20 mL) was added slowly with vigorous stirring. The organic phase was separated from the aqueous phase and washed with water (2 × 70 mL). The organic phase was dried over sodium sulfate, filtered, and concentrated in vacuo to give the product **44** as a clear oil (1.88 g, 95%), which was used in the next step without further purification. R_f = 0.5 (40% acetone/hexane). ^{1}H NMR (500 MHz, CDCl_3): δ 4.62 (br s, 1H, NHCO), 4.24 (t, 2H, CH_2O), 3.16 (m, 2H, CH_2N), 3.01 (s, 3H, CH_3), 1.78 (quin, 2H), 1.59 (quin, 2H), 1.43 (s, 9H).

[4-(4-Hydroxy-butylamino)butyl]carbamic Acid *tert*-Butyl Ester, 45. To a solution of the mesylate **44** (1.88 g, 7 mmol) in acetonitrile (50 mL) at room temperature under N_2 was added a solution of 4-aminobutanol (2.5 g, 28 mmol) in acetonitrile (50 mL) dropwise over 30 min. The reaction mixture was stirred under reflux overnight. The acetonitrile was removed in vacuo, and the oily residue was dissolved in CH_2Cl_2 (100 mL) and washed with 10% aqueous Na_2CO_3 solution (3 × 100 mL). The organic phase was dried over sodium sulfate, filtered, and concentrated in vacuo and the residue purified by flash column chromatography (1:10:89 NH_4-OH:MeOH:CHCl_3) to give the product **45** as a clear oil (1.46 g, 80%), R_f = 0.35 (1:10:89 NH_4OH:MeOH:CHCl_3). ^{1}H NMR (500 MHz, CDCl_3): δ 4.78 (br s, 1H, NHCO), 3.54 (t, 2H, CH_2O), 3.07 (m, 2H), 2.61 (m, 4H, 2 × CH_2), 1.64 (quin, 2H), 1.58 (quin, 2H), 1.48 (m, 4H), 1.42 (s, 9H).

(4-*tert*-Butoxycarbonylamino-butyl)(4-hydroxybutyl)-carbamic Acid *tert*-Butyl Ester, 46. A solution of the mono-BOC alcohol **45** (1.45 g, 5.6 mmol) in methanol (34 mL) and triethylamine (6 mL) was cooled to 0 °C and stirred for 10 min. A solution of di-*tert*-butyl dicarbonate (1.82 g, 8.4 mmol) in methanol (20 mL) was added dropwise over 30 min, and the reaction mixture was stirred overnight under N_2 at room temperature. The methanol and triethylamine were removed in vacuo, and the oily residue was dissolved in CH_2Cl_2 (100 mL) and washed with 0.1 N HCl solution (3 × 80 mL). The CH_2Cl_2 layer was dried over sodium sulfate, filtered, and removed in vacuo to give the product **46** as a clear oil (1.83 g, 91%), which was used in the next step without further purification. R_f = 0.7 (1:10:89 NH_4OH:MeOH:CHCl_3). ^{1}H NMR (500 MHz, CDCl_3): δ 4.67 (m, 1H, NHCO), 3.62 (q, 2H, CH_2O), 3.15 (m, 4H), 3.08 (q, 2H), 1.64−1.38 (m, 26H, 4 × CH_2, 6 × CH_3).

6-[(Anthracen-9-ylmethyl)amino]hexan-1-ol, 48. To a stirred solution of 6-aminohexan-1-ol (0.35 g, 3 mmol) in 25% MeOH/CH_2Cl_2 (10 mL) was added a solution of 9-anthraldehyde **47** (0.52 g, 2.5 mmol) in 25% MeOH/CH_2Cl_2 (10 mL) under N_2. The mixture was stirred at room temperature overnight until the imine formation was complete (monitored by NMR). The solvent was removed in vacuo, the solid residue dissolved in 50% MeOH /CH_2Cl_2 (20 mL), and the solution cooled to 0 °C. NaBH_4 (7.5 mmol) was added in small portions to the solution, and the mixture was stirred at room temperature overnight. The solvent was removed in vacuo, and the solid residue was dissolved in CH_2Cl_2 (30 mL) and washed with 10% aqueous Na_2CO_3 solution (3 × 30 mL). The CH_2Cl_2 layer was dried over anhydrous Na_2SO_4, filtered, and removed in vacuo to give an oily residue. The oil was purified by flash column chromatography (5% MeOH/CHCl_3) to yield the product **48** as a pale yellow solid (0.63 g, 82%), R_f = 0.3 (5% MeOH/CHCl_3). ^{1}H NMR (300 MHz, CDCl_3): δ 8.31 (s, 1H), 8.25 (d, 2H), 7.94 (m, 2H), 7.49 (m, 2H), 7.39 (m, 2H), 4.63 (s, 2H), 3.45 (t, 2H), 2.79 (t, 2H), 1.50 (quin, 2H), 1.43 (quin, 2H), 1.28 (m, 4H). ^{13}C NMR: δ 131.9, 131.8, 130.5, 129.4, 127.4, 126.4, 125.2, 124.3, 62.8, 50.8, 46.1, 33.1, 30.4, 27.5, 26.1. HRMS (FAB) *m/z* calcd for C_21H_26NO (M + H)[+]: 308.2014. Found: 308.2026. Anal. (C_21H_25NO) C, H, N.

Anthracen-9-ylmethyl(6-hydroxyhexyl)carbamic Acid *tert*-Butyl Ester, 49. A solution of the alcohol **48** (0.61 g, 2 mmol) in methanol (17 mL) and triethylamine (3 mL) was cooled to 0 °C and stirred for 10 min. A solution of di-*tert*-

butyl dicarbonate (0.87 g, 3 mmol) in methanol (10 mL) was added dropwise over 30 min, and the reaction mixture was stirred overnight under N_2 at room temperature. The methanol and triethylamine were removed in vacuo, and the oily residue was dissolved in CH_2Cl_2 (50 mL) and washed with 0.1 N HCl solution (3 × 40 mL). The CH_2Cl_2 layer was dried over sodium sulfate, filtered, and removed in vacuo to give the product as a yellow oil (0.78 g, 97%), which was used in the next step without further purification. ^{1}H NMR (300 MHz, CDCl_3): δ 8.38 (m, 3H), 7.94 (m, 2H), 7.49 (m, 2H), 7.42 (m, 2H), 5.50 (s, 2H), 3.41 (t, 2H), 2.78 (m, 2H), 1.57 (s, 9H, CH_3), 1.25 (m, 4H), 0.98 (m, 4H). ^{13}C NMR: δ 156.1, 131.6, 129.4, 129.1, 128.3, 126.5, 125.2, 124.5, 79.9, 62.9, 44.8, 41.3, 32.8, 29.0, 28.6, 26.8, 25.4.

Methanesulfonic Acid 6-(Anthracen-9-ylmethyl-*tert*-butoxycarbonyl-amino)hexyl Ester, 50. A solution of the mono-BOC alcohol **49** (0.78 g, 2 mmol) in anhydrous CH_2Cl_2 (30 mL) and triethylamine (2.9 mmol, 0.4 mL, 1.5 equiv) was cooled to 0 °C. Methanesulfonyl chloride (2.9 mmol, 0.23 mL, 1.5 equiv) was added dropwise and the resulting solution stirred at 0 °C for 4 h and then at room temperature overnight. The reaction mixture was cooled to 0 °C, a 1 M NaOH solution (10 mL) was added slowly to quench the reaction, and the mixture was warmed to room temperature. The aqueous layer was made up to 30 mL with water, and the organic layer was separated off, washed with water (20 mL), and then dried over sodium sulfate. This material was filtered and concentrated in vacuo to give the product **50** as a yellow oil (0.91 g, 97%), which was used in the next step without further purification. ^{1}H NMR (300 MHz, CDCl_3): δ 8.38 (s, 1H), 8.35 (d, 2H), 7.94 (m, 2H), 7.49 (m, 2H), 7.42 (m, 2H), 5.50 (s, 2H), 3.98 (t, 2H), 2.91 (s, 3H), 2.78 (m, 2H), 1.57 (s, 9H, CH_3), 1.38 (m, 2H), 1.18 (m, 2H), 0.95 (m, 4H). ^{13}C NMR: δ 156.1, 131.52, 131.47, 129.5, 128.4, 126.5, 125.3, 124.4, 80.0, 70.3, 56.1, 44.8, 41.3, 37.6, 29.1, 29.0, 28.4, 26.4, 25.1.

[6-(4-Amino-butylamino)hexyl]anthracen-9-ylmethyl-carbamic Acid *tert*-Butyl Ester, 51. To a solution of the mesylate **50** (0.9 g, 1.86 mmol) in anhydrous acetonitrile (10 mL) being stirred at room temperature was added a solution of 1,4-diaminobutane (1.63 g, 18.6 mmol) in anhydrous acetonitrile (10 mL). The reaction mixture was then refluxed overnight. The acetonitrile was removed in vacuo, and the oily residue was dissolved in CH_2Cl_2 (40 mL) and washed with saturated sodium carbonate solution (4 × 40 mL). The CH_2-Cl_2 layer was dried over anhydrous sodium sulfate, filtered, and removed in vacuo to give a yellow oil. The oil was purified by flash column chromatography (1% NH_4OH/10% MeOH/CHCl_3) to yield the product **51** as a yellow oil (0.54 g, 61%), R_f = 0.3 (1% NH_4OH/10% MeOH/CHCl_3). ^{1}H NMR (300 MHz, CDCl_3): δ 8.41 (s, 1H), 8.38 (d, 2H), 7.98 (m, 2H), 7.51 (m, 2H), 7.43 (m, 2H), 5.50 (s, 2H), 2.78 (m, 2H), 2.69 (t, 2H), 2.55 (t, 2H), 2.39 (t, 2H), 1.57 (s, 9H, CH_3), 1.54 (m, 4H), 1.24 (m, 4H), 0.95 (m, 4H). ^{13}C NMR: δ 156.1, 131.5, 129.4, 128.3, 126.5, 125.2, 124.5, 79.8, 50.2, 44.8, 42.5, 41.3, 32.0, 30.3, 28.9, 28.6, 27.9, 27.2, 27.0. HRMS (FAB) *m/z* calcd for C_30H_44N_3O_2 (M + H)[+]: 478.3434. Found: 478.3435.

{4-[(Anthracen-9-ylmethyl)amino]butyl}carbamic Acid *tert*-Butyl Ester, 52. To a stirred solution of amine **40** (0.815 g, 4.3 mmol) in 25% MeOH/CH_2Cl_2 (16 mL) was added a solution of 9-anthraldehyde (0.74 g, 3.6 mmol) in 25% MeOH/CH_2Cl_2 (16 mL) under N_2. The mixture was stirred at room temperature overnight until the imine formation was complete (monitored by NMR). The solvent was removed in vacuo, the solid residue dissolved in 50% MeOH /CH_2Cl_2 (20 mL), and the solution cooled to 0 °C. NaBH_4 (11 mmol) was added in small portions to the solution, and the mixture was stirred at room temperature overnight. The solvent was removed in vacuo, and the solid residue was dissolved in CH_2Cl_2 (50 mL) and washed with 10% aqueous Na_2CO_3 solution (3 × 40 mL). The CH_2Cl_2 layer was dried over anhydrous Na_2SO_4, filtered, and removed in vacuo to give an oily residue. The oil was purified by flash column chromatography (3% MeOH/CHCl_3) to yield the product **52** as a yellow solid (1.31 g, 96%), R_f = 0.4 (3% MeOH/CHCl_3). ^{1}H NMR (300 MHz, CDCl_3): δ 8.35 (s,

1H), 8.28 (d, 2H), 7.95 (d, 2H), 7.50 (m, 2H), 7.41 (m, 2H), 4.75 (br s, 1H, NHCO), 4.68 (s, 2H), 3.10 (q, 2H), 2.83 (t, 2H), 1.55 (m, 4H), 1.41 (m, 9H, CH$_3$). ^{13}C NMR: δ 156.1, 131.9, 131.7, 130.4, 129.3, 127.3, 126.3, 125.1, 124.3, 79.2, 50.4, 46.1, 40.8, 28.8, 28.2, 27.8. HRMS (FAB) m/z calcd for C$_{24}$H$_{31}$N$_2$O$_2$ (M + H)$^+$: 379.2386. Found: 379.2373. Anal. (C$_{24}$H$_{30}$N$_2$O$_2$·0.2H$_2$O) C, H, N.

{4-[Anthracen-9-ylmethyl(3-cyanopropyl)amino]butyl}-carbamic Acid *tert*-Butyl Ester, 53. To a solution of the secondary amine **52** (1.16 g, 3.1 mmol) in anhydrous acetonitrile (40 mL) were added potassium carbonate (1.27 g, 9.2 mmol) and 4-bromobutyronitrile (0.91 g, 0.61 mL, 6.1 mmol), and the resulting mixture was refluxed overnight. The mixture was filtered to remove most of the inorganic salts, and the acetonitrile was removed in vacuo to give a solid/oily residue, which was purified by flash column chromatography (gradient of CHCl$_3$ up to 1% MeOH/CHCl$_3$) to yield the product **53** as a yellow oil (0.99 g, 73%), R_f = 0.35 (1% MeOH/CHCl$_3$). ^{1}H NMR (300 MHz, CDCl$_3$): δ 8.38 (m, 3H), 7.95 (d, 2H), 7.50 (m, 2H), 7.41 (m, 2H), 4.48 (br s, 1H), 4.47 (s, 2H), 3.02 (q, 2H), 2.57 (t, 2H), 2.50 (t, 2H), 1.90 (t, 2H), 1.59 (m, 4H), 1.43 (m, 9H, CH$_3$), 1.39 (m, 2H). ^{13}C NMR: δ 156.2, 131.6, 131.4, 130.1, 129.4, 127.9, 126.0, 125.1, 124.9, 120.1, 79.4, 54.4, 51.8, 51.4, 40.6, 28.9, 28.5, 24.4, 24.2, 14.9. HRMS (FAB) m/z calcd for C$_{28}$H$_{36}$N$_3$O$_2$ (M + H)$^+$: 446.2808. Found: 446.2832. Anal. (C$_{28}$H$_{35}$N$_3$O$_2$·0.8H$_2$O) C, H, N.

{4-[(4-Aminobutyl)anthracen-9-ylmethyl-amino]butyl}-carbamic Acid *tert*-Butyl Ester, 54. In a thick-walled glass jar compatible with the Parr shaker, nitrile **53** (0.8 g, 1.8 mmol) was dissolved in ethanol (40 mL), and concentrated aqueous NH$_4$OH (4 mL) was added along with Raney nickel (3 g). Ammonia gas was bubbled for 5 min through the mixture, which was precooled to 0 °C. The yellow mixture was attached to a Parr shaker, and hydrogen gas (75 psi) was introduced after a brief evacuation of the headspace. After 18 h, TLC (1% MeOH/CHCl$_3$) revealed complete conversion of the nitrile. The mixture was filtered and the filtrate concentrated under vacuum to give a yellow oil. The oil was dissolved in CH$_2$Cl$_2$ (50 mL) and washed with 10% aqueous Na$_2$CO$_3$ solution (3 × 40 mL). The CH$_2$Cl$_2$ layer was dried over anhydrous Na$_2$SO$_4$, filtered, and removed in vacuo to give the product **54** as a yellow oil (0.71 g, 88%), which was used in the next step without further purification. ^{1}H NMR (300 MHz, CDCl$_3$): δ 8.46 (d, 2H), 8.33 (s, 1H), 7.95 (d, 2H), 7.42 (m, 4H), 4.50 (m, NHCO, 1H), 4.45 (s, 2H), 2.88 (q, 2H), 2.43 (m, 6H), 1.56–1.37 (m, 11H), 1.24 (m, 6H). ^{13}C NMR: δ 156.1, 131.6, 131.5, 131.0, 129.2, 127.5, 125.6, 125.4, 125.0, 79.2, 53.8, 53.5, 51.5, 42.3, 40.6, 32.0, 28.8, 28.2, 24.6. HRMS (FAB) m/z calcd for C$_{28}$H$_{40}$N$_3$O$_2$ (M + H)$^+$: 450.3121. Found: 450.3133.

Anthracen-9-ylmethyl-(4-{4-[(anthracen-9-ylmethyl)-amino]butylamino}butyl)carbamic Acid *tert*-Butyl Ester, 56. To a stirred solution of 9-anthraldehyde **47** (0.098 g, 0.47 mmol) in 25% MeOH/CH$_2$Cl$_2$ (5 mL) at 0 °C was added a solution of the mono-BOC diamine **55** (0.21 g, 0.47 mmol) in 25% MeOH/CH$_2$Cl$_2$ (5 mL) under N$_2$. The mixture was stirred at room temperature overnight until the imine formation was complete (monitored by NMR). The solvent was removed in vacuo, the solid residue dissolved in 50% MeOH/CH$_2$Cl$_2$ (10 mL), and the solution cooled to 0 °C. NaBH$_4$ (1.4 mmol) was added in small portions to the solution, and the mixture was stirred at room temperature overnight. The solvent was removed in vacuo, and the oily/solid residue was dissolved in CH$_2$Cl$_2$ (25 mL) and washed with 10% aqueous Na$_2$CO$_3$ solution (3 × 25 mL). The CH$_2$Cl$_2$ layer was dried over anhydrous Na$_2$SO$_4$, filtered, and removed in vacuo to give an oily residue. The oil was purified by flash column chromatography (0.5% NH$_4$OH/5% MeOH/CHCl$_3$) to yield the product **56** as a yellow oil (0.2 g, 67%), R_f = 0.25 (0.5% NH$_4$OH/5% MeOH/CHCl$_3$). ^{1}H NMR (300 MHz, CDCl$_3$): δ 8.33 (m, 6H), 7.94 (d, 4H), 7.49 (t, 4H), 7.41 (t, 4H), 5.48 (s, 2H), 4.67 (s, 2H), 2.84 (t, 2H), 2.75 (m, 2H), 2.36 (t, 2H), 2.16 (t, 2H), 1.70–1.48 (m, 11H), 1.41 (m, 2H), 1.21 (m, 2H), 1.04 (m, 2H). ^{13}C NMR: δ 156.2, 132.0, 131.7, 131.5, 130.4, 129.5, 129.4, 129.1, 128.4, 127.4, 126.5, 126.3, 125.22, 125.15, 124.3, 80.0, 50.8,

50.0, 49.6, 46.2, 44.8, 41.3, 29.0, 28.4, 28.3, 27.5, 26.6. HRMS (FAB) m/z calcd for C$_{43}$H$_{50}$N$_3$O$_2$ (M + H)$^+$: 640.3903. Found: 640.3894.

Supporting Information Available: Elemental data for compounds **12**, **13**, **15–19**, **24**, **26–28**, **33**, **37–39**, **48**, **52**, and **53**. This material is available free of charge via the Internet at http://pubs.acs.org.

References

(1) (a) Cullis, P. M.; Green, R. E.; Merson-Davies, L.; Travis, N. Probing the mechanism of transport and compartmentalisation of polyamines in mammalian cells. *Chem. Biol.* **1999**, *6*, 717–729 and references therein. (b) Seiler, N.; Dezeure F. Polyamine transport in mammalian cells. *Int. J. Biochem.* **1990**, *22*, 211–218. (c) Seiler, N.; Delcros J.-G.; Moulinoux, J. P. Polyamine Transport in Mammalian Cells. An Update. *Int. J. Biochem. Cell Biol.* **1996**, *28*, 843–861.

(2) Phanstiel, O., IV; Price, H. L,; Wang, L.; Juusola, J.; Kline, M.; Shah, S. M. The Effect of Polyamine Homologation on the Transport and Cytotoxicity Properties of Polyamine−(DNA-Intercalator) Conjugates. *J. Org. Chem.* **2000**, *65*, 5590–5599.

(3) Wang, L.; Price, H. L.; Juusola, J.; Kline, M.; Phanstiel, O., IV. The Influence of Polyamine Architecture on the Transport and Topoisomerase II Inhibitory Properties of Polyamine DNA−Intercalator Conjugates. *J. Med. Chem.* **2001**, *44*, 3682–3691.

(4) Wang, C.; Delcros, J.-G.; Biggerstaff, J.; Phanstiel, O., IV. Synthesis and Biological Evaluation of N^1-(Anthracen-9-ylmethyl)triamines as Molecular Recognition Elements for the Polyamine Transporter. *J. Med. Chem.* **2003**, *46*, 2663–2671.

(5) Wang, C.; Delcros, J.-G.; Biggerstaff, J.; Phanstiel, O., IV. Molecular Requirements for Targeting the Polyamine Transport System: Synthesis and Biological Evaluation of Polyamine−Anthracene Conjugates. *J. Med. Chem.* **2003**, *46*, 2672–2682.

(6) Wang, C.; Delcros, J.-G.; Cannon, L.; Konate, F.; Carias, H.; Biggerstaff, J.; Gardner, R. A.; Phanstiel, O., IV. Defining the Molecular Requirements for the Selective Delivery of Polyamine Conjugates into Cells Containing Active Polyamine Transporters. *J. Med. Chem.* **2003**, *46*, 5129–5138.

(7) (a) Bergeron, R. J.; Feng, Y.; Weimar, W. R.; McManis, J. S.; Dimova, H.; Porter, Carl; Raisler, B.; Phanstiel, O. A Comparison of Structure−Activity Relationships between Spermidine and Spermine Analogue Antineoplastics. *J. Med. Chem.* **1997**, *40*, 1475–1494. (b) Kramer, D. L.; Miller, J. T.; Bergeron, R. J.; Khomutov, R.; Khomutov, A.; Porter, C. W. Regulation of polyamine transport by polyamines and polyamine analogues. *J. Cell. Physiol.* **1993**, *155*, 399–407.

(8) (a) Nagarayan, M.; Xiao, X.; Antony, S.; Kohlhagen, G.; Pommier, Y.; Cushman, M. Design, Synthesis, and Biological Evaluation of Indenoisoquinoline Topoisomerase I Inhibitors Featuring Polyamine Side Chains on the Lactam Nitrogen. *J. Med. Chem.* **2003**, *46*, 5712–5724. (b) Pietrangeli, P.; Nocera, S.; Mondova, B.; Morpurgo, L. Is the catalytic mechanism of bacteria, plant, and mammal copper-TPQ amine oxidases identical? *Biochim. Biophys. Acta* **2003**, *1647*, 152–156.

(9) Bergeron, R. J.; McManis, J. S.; Franklin, A. M.; Yao, H.; Weimar. W. R. Polyamine−Iron Chelator Conjugate. *J. Med. Chem.* **2003**, *46*, 5478–5483.

(10) (a) Williams, J. I.; Weitman, S.; Gonzalez, C. M.; Jundt, C. H.; Marty, J.; Stringer, S. D.; Holroyd, K. J.; McLane, M. P.; Chen, Q.; Zasloff, M.; Von Hoff, D. D. Squalamine Treatment of Human Tumors in *nu/nu* Mice Enhances Platinum-based Chemotherapies. *Clin. Cancer Res.* **2001**, *7*, 724–733. (b) Bhargava, P.; Marshall, J. L.; Dahut, W.; Rizvi, N.; Trocky, N.; Williams, J. I.; Hait, H.; Song, S. Holroyd, K. J.; Hawkins, M. J. A Phase I and Pharmacokinetic Study of Squalamine, a Novel Antiangiogenic Agent, in Patients with Advanced Cancers. *Clin. Cancer Res.* **2001**, *7*, 3912–3919.

(11) (a) Bergeron, R. J.; Wiegand, J.; McManis, J. S.; Weimar, W. R.; Smith, R. E.; Algee, S. E.; Fannin, T. L.; Slusher, M. A.; Snyder, P. S. Polyamine Analogue Antidiarrheals: A Structure−Activity Study. *J. Med. Chem.* **2001**, *44*, 232–244. (b) Bergeron, R. J.; Yao, G. W.; Yao, H.; Weimar, W. R.; Sninsky, C. A.; Raisler, B.; Feng, Y.; Wu, Q.; Gao, F. Metabolically Programmed Polyamine Analogue Antidiarrheals. *J. Med. Chem.* **1996**, *39*, 2461–2471. (c) Bergeron, R. J.;; Neims, A. H.; McManis, J. S.; Hawthorne, T. R.; Vinson, J. R. T.; Bortell, R.; Ingeno, M. J.

Synthetic polyamine analogues as antineoplastics. *J. Med. Chem.* **1988**, *31*, 1183−1190. (d) Casero, R. A., Jr.; Woster, P. M. Terminally Alkylated Polyamine Analogues as Chemotherapeutic Agents. *J. Med. Chem.* **2001**, *44*, 1−26 and references therein.

(12) Delcros, J.-G.; Tomasi, S.; Carrington, S.; Martin, B.; Renault, J.; Blagbrough, I. S.; Uriac, P. Effect of spermine conjugation on the cytotoxicity and cellular transport of acridine. *J. Med. Chem.* **2002**, *45*, 5098−5111.

(13) Azzam, T.; Eliyahu, H.; Shapira, L.; Linial, M.; Barenholz, Y.; Domb, A. J. Polysaccharide−Oligoamine Based Conjugates for Gene Delivery. *J. Med. Chem.* **2002**, *45*, 1817−1824.

(14) Stark, P. A.; Thrall, B. D. Meadows, G. G.; Abdul-Monem M. M. Synthesis and Evaluation of Novel Spermidine Derivatives as Targeted Cancer Chemotherapeutic Agents. *J. Med. Chem.* **1992**, *35*, 4264−4269.

(15) Cohen, G. M.; Cullis, P.; Hartley, J. A.; Mather, A. Symons, M. C. R.; Wheelhouse, R. T. Targeting of Cytotoxic Agents by Polyamines: Synthesis of a Chloroambucil-Spermidine Conjugate. *J. Chem. Soc., Chem. Commun.* **1992**, 298−300.

(16) Cai, J.; Soloway, A. H., Synthesis of Carboranyl Polyamines for DNA Targeting. *Tetrahedron Lett.* **1996**, *37*, 9283−9286.

(17) Ghaneolhosseini, H.; Tjarks, W.; Sjoberg, S. Synthesis of Novel Boronated Acridines and Spermidines as Possible Agents for BNCT. *Tetrahedron* **1998**, *54*, 3877−3884.

(18) Blagbrough, I. S.; Geall, A. J. Homologation of Polyamines in the Synthesis of Lipo-Spermine Conjugates and Related Lipoplexes. *Tetrahedron Lett.* **1998**, *39*, 443−446.

(19) Cullis, P. M.; Merson-Davies, L.; Weaver, R. Conjugation of a Polyamine to the Bifunctional Alkylating Agent Chlorambucil Does Not Alter the Preferred Cross-Linking Site in Duplex DNA. *J. Am. Chem. Soc.* **1995**, *117*, 8033−8034.

(20) Aziz, S. M.; Yatin, M.; Worthen, D. R.; Lipke, D. W.; Crooks, P. A. A novel technique for visualising the intracellular localization and distribution of transported polyamines in cultured pulmonary artery smooth muscle cells. *J. Pharm. Biomed. Anal.* **1998**, *17*, 307−320.

(21) Saab, N. H.; West, E. E.; Bieszk, N. C.; Preuss, C. V.; Mank, A. R.; Casero, R. A.; Woster P. M. Synthesis and Evaluation of Polyamine Analogues as Inhibitors of Spermidine/Spermine-N^1-Acetyltransferase (SSAT) and as Potential Antitumor Agents. *J. Med. Chem.* **1993**, *36*, 2998−3004.

(22) (a) Porter, C. W.; Cavanaugh, P. F.; Ganis, B.; Kelly, E.; Bergeron, R. J. Biological properties of N-4 and N-1, N-8-spermidine derivatives in cultured L1210 leukemia cells. *Cancer Res.* **1985**, *45*, 2050−2057. (b) Porter, C. W.; Bergeron, R. J.; Stolowich, N. J. Biological properties of N4-spermidine derivatives and their potential in anticancer chemotherapy. *Cancer Res.* **1982**, *42*, 4072−4078.

(23) Bergeron, R. J.; McManis, J. S.; Weimar, W. R.; Schreier, K. M.; Gao, F.; Wu, Q.; Ortiz-Ocasio, J.; Luchetta, G. R.; Porter, C.; Vinson, J. R. T. The role of charge in polyamine analogue recognition. *J. Med. Chem.* **1995**, *38*, 2278−2285.

(24) Porter, C.; Miller, J.; Bergeron, R. J. Aliphatic chain-length specificity of the polyamine transport system in ascites L1210 leukemia cells. *Cancer Res.* **1984**, *44*, 126−128.

(25) Xia, C. Q.; Yang, J. J.; Ren, S.; Lien, E. J. QSAR analysis of polyamine transport inhibitors in L1210 cells. *J. Drug Targeting* **1998**, *6*, 65−77.

(26) O'Sullivan, M. C.; Golding, B. T.; Smith, L. L.; Wyatt, I. Molecular features necessary for the uptake of diamines and related compounds by the polyamine receptor of rat lung slices. *Biochem. Pharmacol.* **1991**, *41*, 1839−1848.

(27) Bergeron, R. J.; McManis, J. S.; Liu, C. Z.; Feng, Y.; Weimar, W. R.; Luchetta, G. R.; Wu, Q.; Ortiz-Ocasio, J.; Vinson, J. R. T.; Kramer, D.; Porter, C. Antiproliferative Properties of Polyamine Analogues: A Structure−Activity Study. *J. Med. Chem.* **1994**, *37*, 3464−3476.

(28) Soulet, D.; Covassin, L.; Kaouass, M.; Charest-Gaudreault, R.; Audette, M.; Poulin, R. Role of endocytosis in the internalisation of spermidine-C2-BODIPY, a highly fluorescent probe of polyamine transport. *Biochem. J.* **2002**, *367*, 347−357.

(29) Burns, M. R.; Carlson, C. L.; Vanderwerf, S. M.; Ziemer, J. R.; Weeks, R. S.; Cai, F.; Webb, H. K.; Graminski, G. F. Amino Acid/ Spermine Conjugates: Polyamine Amides as Potent Spermidine Uptake Inhibitors. *J. Med. Chem.* **2001**, *44*, 3632−3644.

(30) (a) Kumar, C. V.; Asuncion, E. H. DNA Binding Studies and Site Selective Fluorescence Sensitization of an Anthryl Probe. *J. Am. Chem. Soc.* **1993**, *115*, 8547−8553. (b) Rodger, A.; Taylor, S.; Adlam, G.; Blagbrough, I. S.; Haworth, I. S. Multiple DNA Binding Modes of Anthracene-9-Carbonyl-N^1-Spermine. *Bioorg. Med. Chem.* **1995**, *3*, 861−872.

(31) Wang, C.; Abboud, K. A.; Phanstiel, O., IV. Synthesis and Characterization of N^1-(4-Toluenesulfonyl)-N^1-(9-anthracenemethyl)triamines. *J. Org. Chem.* **2002**, *67*, 7865−7868.

(32) Blagbrough, I. S.; Geall, A. J. Practical Synthesis of Unsymmetrical Polyamine Amides. *Tetrahedron Lett.* **1998**, *39*, 439−442.

(33) Kuksa, V.; Buchan, R.; Lin, P. K. T. Synthesis of Polyamines, Their Derivatives, Analogues and Conjugates. *Synthesis* **2000**, No. 9, 1189−1207.

(34) Zaragoza, F. One-Step Conversion of Alcohols into Nitriles with Simultaneous Two-Carbon Chain Elongation. (Cyanomethyl)-trimethylphosphonium iodide as reagent with a dual mode of action. *J. Org. Chem.* **2002**, *67*, 4963−4964.

(35) Gardner, R. A.; Kinkade, R.; Wang, C.; Phanstiel, O., IV. Total Synthesis of Petrobactin and Its Homologues as Potential Growth Stimuli for *Marinobacter hydrocarbonoclasticus*, an Oil-Degrading Bacteria. *J. Org. Chem.* **2004**, *69*, 3530−3537.

(36) Martin, B.; Possémé, F.; Le Barbier, C.; Carreaux, F.; Carboni, B.; Seiler, N.; Moulinoux, J.-P.; Delcros, J.-G. *N*-Benzylpolyamines as Vectors of Boron and Fluorine for Cancer Therapy and Imaging: Synthesis and Biological Evaluation. *J. Med. Chem.* **2001**, *44*, 3653−3664.

(37) Mandel, J. L.; Flintoff, W. F. Isolation of mutant mammalian cells altered in polyamine transport. *J. Cell. Physiol.* **1978**, *97*, 335−344.

(38) Byers, T. L.; Wechter, R.; Nuttall, M. E.; Pegg, A. E. Expression of a human gene for polyamine transport in Chinese hamster ovary cells. *Biochem. J.* **1989**, *263*, 745−752.

(39) Mosmann, T. Rapid colorimetric assay for cellular growth and survival: application to proliferation and cytotoxicity assays. *J. Immunol. Methods* **1983**, *65*, 55−63.

(40) Clément, S.; Delcros, J. G.; Feuerstein, B. G. Spermine uptake is necessary to induce haemoglobin synthesis in murine erythroleukemia cells. *Biochem. J.* **1995**, *312*, 933−938.

(41) Cheng, Y. C.; Prusoff, W. H. Relationship between the inhibition constant (Ki) and the concentration of inhibitor which causes 50% inhibition (IC50) of an enzymatic reaction. *Biochem. Pharmacol.* **1973**, *22*, 3099−3108.

(42) Covassin, L.; Desjardins, M.; Charest-Gaudreault, R.; Audette, M.; Bonneau, M. J.; Poulin, R. Synthesis of spermidine and norspermidine dimers as high affinity polyamine transport inhibitors. *Bioorg. Med. Chem. Lett.* **1999**, *9*, 1709−1714.

(43) Torossian, K.; Audette, M.; Poulin, R. Substrate protection against inactivation of the mammalian polyamine transport system by 1-ethyl-3-(3-dimethylaminopropyl)carbodiimide. *Biochem. J.* **1996**, *319*, 21−26.

(44) Bergeron, R. J.; Müller, R.; Bussenius, J.; McManis, J. S.; Merriman, R. L.; Smith, R. E.; Yao, H.; Weimar, W. R. Synthesis and Evaluation of Hydroxylated Polyamine Analogues as Antiproliferatives. *J. Med. Chem.* **2000**, *43*, 224−235.

(45) Lowry, O. H.; Rosenbraugh, N. J.; Farr, A. L.; Randall, R. J. Protein Measurement with the Folin Phenol Reagent. *J. Biol. Chem.* **1951**, *193*, 265−275.